Fall 2011

The origin of quartz glomerocrysts: insights from the rhyolite dike at Medicine Park, OK

Sedeg Ahmed E. Ahmed

Department:

THE ORIGIN OF QUARTZ GLOMEROCRYSTS: INSIGHTS FROM THE RHYOLITE DIKE AT MEDICINE PARK, OK

by

SEDEG AHMED E. AHMED

A THESIS

Presented to the Faculty of the Graduate School of the

MISSOURI UNIVERSITY OF SCIENCE AND TECHNOLOGY

In Partial Fulfillment of the Requirements for the Degree

MASTER OF SCIENCE IN GEOLOGY AND GEOPHYSICS

2011

Approved by

John P. Hogan, Advisor

Cheryl Seeger

David J. Wronkiewicz

ABSTRACT

The origin of quartz glomerocrysts a distinctive petrographic feature of the rhyolite dike in Medicine Park, Oklahoma, was investigated using transmitted light and cathodoluminescence microscopy to determine if quartz glomerocrysts formed during quartz crystallization or during quartz dissolution. Quartz glomerocrysts are typically comprised of two to six individual phenocrysts of quartz and commonly exhibit subhedral partially embayed crystal forms with very rare euhedral phenocrysts in both glomerocrysts and individual quartz phenocrysts. The size range of the individual quartz phenocrysts are 0.08mm to 1.7mm while the size range is 0.08mm to 3.25mm for quartz glomerocrysts . Cathodoluminescence revealed that individual quartz phenocrysts which comprise glomerocrysts showed abrupt truncation of internal compositional growth zonation along the shared resorbed crystal surfaces, demonstrating the quartz glomerocrysts formed after initiation of quartz dissolution. The driving force behind quartz dissolution is consistent with decompression during magma ascent resulting in a decrease in the stability field for quartz due to the shift in the position of the coetectic in the system Q-Ab-Or-H_2O. Juxtaposition of dissolving quartz phenocrysts during magma ascent leads to the formation of glomerocrysts as a result of crystallization of the overlapping boundary layer melts that surround the dissolving quartz phenocrysts. The common occurrence of glomerophyric quartz phenocrysts in granites, akin to those observed in the rhyolite dike, may have also formed as a result of decompression dissolution, thus providing a textural record of magmatic ascent.

ACKNOWLEDGMENTS

First of all, I praise Almighty Allah for his blessings, grace and guidance. I would like to express my thanks to my advisor Dr. John Hogan for his support, guidance and patience throughout this project.

I would like to express my heartfelt gratitude to my parents, all my family members and my fiancée for their support and invocations. I would also like to extend my appreciations to the members of my committee, Dr. Cheryl Seeger and Dr. David J. Wronkiewicz for their encouragement and insightful comments.

My particular gratitude is also extended to Dr. Sheila Seaman for her contributions. A successful completion of this work would not have been possible without her help. I also thank the fellow graduate students, the faculty and the staff at the Geological Sciences and Engineering department for their help through my Masters.

TABLE OF CONTENTS

Page

LIST OF ILLUSTRATIONS

LIST OF TABLES

1. INTRODUCTION

In North America, the Southern Oklahoma Aulacogen is one of the best preserved and best exposed examples of Cambrian age rift-related igneous activity (Hoffman et al. 1974). Exposed rocks consist of mafic plutonic and felsic volcanic and plutonic rocks (Gilbert and Myers, 1986). Numerous basaltic dikes and rare "rhyolite" dikes crosscut members of the Wichita Granite Group and represent the final stages of igneous activity. The rhyolite dikes are porphyritic intrusive igneous rocks with quartz and feldspar phenocrysts set in a fine grained groundmass of quartz and feldspar. The porphyritic texture reflects a rapid increase in the cooling rate of the magma during crystallization that can be attributed to intrusion of the partially crystallized magma into relatively cold Rush Lake Granite at shallow levels in the crust.

A distinctive texture of the rhyolite dike at Medicine Park, Oklahoma, as well as many other rhyolites and granites worldwide, is the presence of quartz and alkali feldspar glomerocrysts. This study focusses on the origin of the quartz glomerocrysts. The origin of the alkali feldspar glomerocrysts will discussed at a later date. The quartz glomerocrysts are typically comprise two to six individual phenocrysts of quartz and commonly exhibit subhedral partially embayed crystal forms with very rare euhedral phenocrysts in both glomerocrysts and individual quartz phenocrysts. The origin of this texture has been attributed to the process of "synneusis," the attachment of crystals along planar crystallographic faces during crystallization (Vance, 1969) and alternatively suggested to form during mineral dissolution as the result of crystallization of

overlapping boundary layer melts that form adjacent to dissolving crystals (Hogan, 1993).

This study reports the results of a transmitted light and cathodoluminescence (CL) investigation of quartz glomerocrysts in the rhyolite dike of Medicine Park, Oklahoma. Quartz can preserve a detailed growth history in the fine scale internal zoning observable by variations in CL intensity attributed to variation in trace abundances of aluminum, alkalis, and transition elements (Sprunt 1981, Perny et al. 1992; Gotze et al. 2001). In igneous rocks, CL has been successfully used to show growth styles and alteration structures reflecting crystallization history of the magma and subsolidus annealing (Muller et al. 2010). However, caution must be used in interpreting textures in plutonic rocks, such as granites, as the earlier stages of crystal growth for some minerals may be either poorly recorded or overprinted in the final plutonic rock by processes occurring late in crystallization or by the subsequent cooling history of the rock (Higgins, 1998; Schaeben et al. 2002). The investigation of the rhyolite dike mitigates these concerns as the crystallization of the dike was arrested by quenching, thus preserving the early history of "granite" crystallization and minimizing subsolidus re-equilibration associated with slow cooling plutonic rocks. The character of the internal zoning of individual quartz crystals which form the glomerocrysts will help to determine if the glomerocrysts formed during quartz crystallization (i.e., synneusis) or during quartz dissolution (i.e., resorption aggregation).

1.1. GEOLOGICAL SETTING OF THE WICHITA MOUNTAINS

The Southern Oklahoma Aulacogen (SOA) is among many aulacogens that formed during the breakup of the Laurentian Supercontinent during the late Proterozoic

to early Cambrian time (Hoffman et al. 1974) (Fig. 1.1). Igneous rocks associated with the aulacogen were subsequently buried beneath Paleozoic sediments and later uplifted by block faulting during the Pennsylvanian to form the Arbuckle Mountains in southern Oklahoma and the Wichita Mountains in southwestern Oklahoma (Gilbert, 1983). Igneous activity associated with rifting that formed the SOA occurred in two separate stages. In the early stage, mafic magma was dominant as a gabbroic magma intrusion, while in the later stage, felsic magma is dominant as rhyolite extrusion and intrusion of large sheet granites (Gilbert and Hughes, 1986).

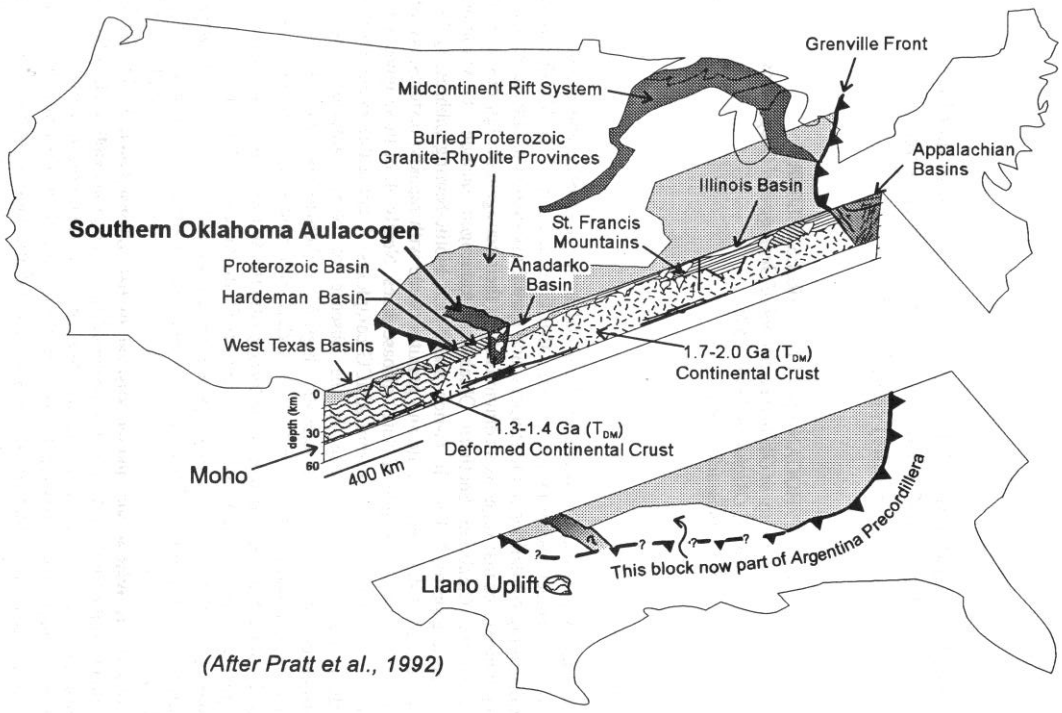

Figure 1.1. Location of Southern Oklahoma Aulacogen Related to the Mid-Continent Grenville Front (Hogan and Gilbert, 1998).

Gilbert and Hogan (2010) recently summarized the regional geology and age relationships of igneous rocks cropping out in the Wichita Mountains (Fig. 1.2). The Glen Mountains Layered Complex (GMLC) of the Raggedy Mountains Gabbro Group (RMGG) is the oldest exposed outcrop of SOA (Ham et al., 1964; Powell et al. 1980). The GMLC is a layered anorthositic gabbro complex that spreads through an area at least 2000km^2. The age dating study of GMLC (Lambert et al. 1988) yielded ages of 577±165 Ma by using Rb-Sr isochron age and 528±29Ma by using Sm-Nd. The GMLC consists of three main units which are respectively plagioclase-olivine-pyroxene, plagioclase-pyroxene and plagioclase cumulate in outcrop. The GMLC is intruded by hydrous biotite-bearing gabbro plutons less than 20 km^2 indiameter as well as gabbroic dikes of the Roosevelt Gabbro Group. A geochronological study of biotite and amphibole from the Roosevelt Gabbro determined $^{40}Ar/^{39}Ar$ recorded ages of 535±8 Ma (late amphibole from a pegmatite), 533±2 Ma (amphibole from the gabbro) and 533±4 (biotite from the gabbro) (Hames et al.1995).

Felsic igneous rocks of the SOA are characterized by high-silica magmas that initially formed the Cartlon Rhyolite Group (CRG) and by intrusion of subvolcanic A-type sheet granites of the Wichita Granite Group (WGG). The CRG is extensive and comprises a thick sequence, up to 1.4 km thick, covering a 44,000 km^2 area with subaerial flows, minor ignimbrites, non-marine air-fall tuff agglomerates and rare basalt flows (Ham et al. 1964). The CRG is an A- type porphyritic rhyolite with phenocrysts of alkali-feldspar, lesser plagioclase, oxides and resorbed quartz. The groundmass consists of feldspar, quartz and oxides (Ham et al. 1964). The age of CRG is 525±25 Ma using U-Pb dating of zircon from the Quanah Granite (Tilton et al. 1962). The recent age dating

study in a resulted relatively short time period between 530±1.5 and 533±1.5 Ma for the granites and rhyolites as well (Wright et al. 1996).

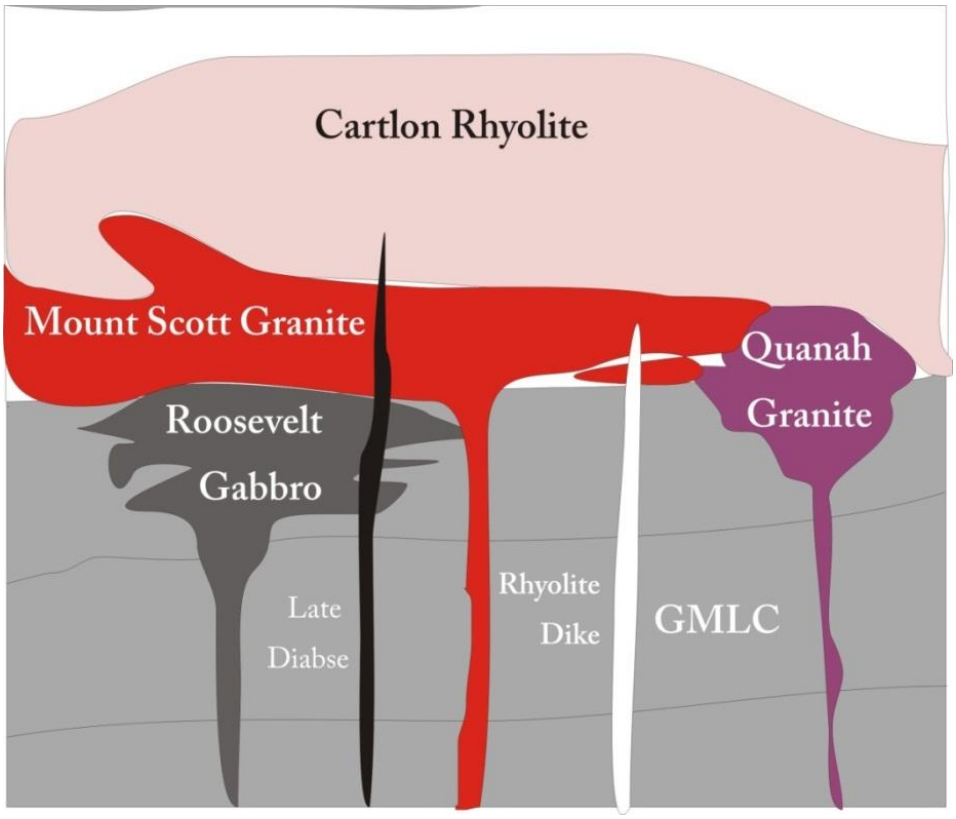

Figure 1.2. Schematic Cross-Section of the Relationship of the Major Igneous Units of the SOA. GMLC is Glen Mountains Layered Complex (After Price 1998).

Members of the WGG appear to be localized along the regional angular unconformity between the GMLC and the CRG (Ham et al. 1964; Hogan and Gilbert, 1997). The Mount Scott is the largest granite sheet of the WGG. It extends over an area of 55 km length and 17 km width with a thickness of 0.5 km (Merritt et al. 1965; Hogan

and Gilbert, 1995). The Mount Scott Granite sheet spread out and crystallized along the angular unconformity between the CRG and the GMLC (Ham et al. 1964; Hogan and Gilbert, 1995). The WGG members are typically leucogranitic alkali feldspar granites (Gilbert and Myers, 1986). The WGG granites have been separated into medium-grained (1-5 mm) (Reformatory and Quanah Granites) and fine-grained (< 1 mm) (Mount Scott) (Hogan and Gilbert, 1997). Even though the majority of the granite members have seriate texture, porphyritic textures are still common. The Mount Scott Granite is recognized by the presence of ovoid anorthoclase phenocrysts rimmed by plagioclase (i.e., rapakivi texture) set in a finer grained groundmass (Price et al. 1996). The age dating of the older unit in WGG (Mount Scott Granite) is 535 ± 3 Ma using U-Pb dating of zircon (Hogan and Gilbert, 1995).

Diabase and rhyolite dikes have intruded the SOA as a last stage of igneous activity in mid-continent rift events (Ham et al. 1964; Gilbert and Hughes, 1986). The diabase dikes are Fe and Ti-rich tholeiites with "within-plate" trace element characteristics (Weaver et al. 1986). While the diabase dikes are common throughout the Wichita Mountains, rhyolite dikes (one of which is the subject of this investigation) are rare.

1.2. GEOLOGICAL SETTING OF THE RHYOLITE DIKE OF MEDICINE PARK

The rhyolite dike of Medicine Park is well exposed in a road cut along US Hwy. 49 immediately north of the Medicine Park State Fish Hatchery (Price 1998; Hogan and O'Donnell, 2008). The rhyolite dike was considered a late stage dike of the SOA by Ham et al. (1964). The tectonic significance of the rhyolite dike was emphasized by Gilbert and Myers (1986) and Gilbert and Powell (1988) in that the rhyolite dike intrudes the

Rush Lake Granite, thus recording a period of uplift and removal of the CRG and a portion of the Mount Scott Granite before magmatism associated with the SOA completely ceased. The intrusive contact between the rhyolite dike and Rush Lake Granite, a member of WGG, is well defined (Price, 1998). The east side of the rhyolite dike shows fingering into the Rush Lake Granite while the west side of the dike shows a sharp, irregular intrusive contact with the granite (Gilbert and Powell, 1988).

2. METHODS

Detailed petrographic observations of the rhyolite dike were initially made on cut polished slabs using a stereo zoom microscope. These observations were used to identify the different textural modes of quartz in the rhyolite dike (see Appendix A). Based upon these observations, thin section blanks were cut from the polished slabs and polished thin sections were prepared by Burnham Petrographics LLC. The textural variety in the occurrence of quartz was further refined in transmitted light using a polarizing microscope. Based upon transmitted light observations, selected thin sections were sent to Dr. Shelia Seaman of the University of Massachusetts for investigation using the CL technique (see Appendix B). CL has the ability to image subtle internal compositional variations which reflect growth zoning in quartz that is not visible in transmitted light microscopy (see Gotze et al. 2001 for a review of CL in quartz).

3. RESULTS

3.1. POLISHED SLABS

The rhyolite dike exhibits a porphyritic texture (Fig. 3.1). The phenocryst assemblage consists of subhedral to euhedral salmon colored alkali-feldspar phenocrysts and subhedral to anhedral grey quartz phenocrysts set in a very fine grained red matrix of interlocking alkali feldspar and quartz. Alkali feldspar and quartz occur both as glomerocrysts and as individual phenocrysts. The phenocrysts comprise about 20% of the rhyolite dike; 60% of the phenocrysts are alkali feldspar and the other 40% are quartz. The size range of the individual quartz phenocrysts are 0.08mm to 1.7mm, while the range of size is 0.08mm to 3.25mm for quartz glomerocrysts. Open void spaces in the rhyolite dike are common.

3.2. TRANSMITTED LIGHT MICROSCOPY

Petrographic analysis of quartz phenocrysts in the rhyolite dikes show a variety of morphologies including: 1) rare euhedral crystals, 2) abundant subhedral crystals with irregular embayed edges and 3) clusters of two to six quartz crystals (Figs. 3.2 and 3.3). Quartz phenocrysts were categorized on the basis of different textural features (e.g., size, shape) as well as spatial association (inclusion in alkali feldspar, isolated phenocrysts, glomerocrysts).

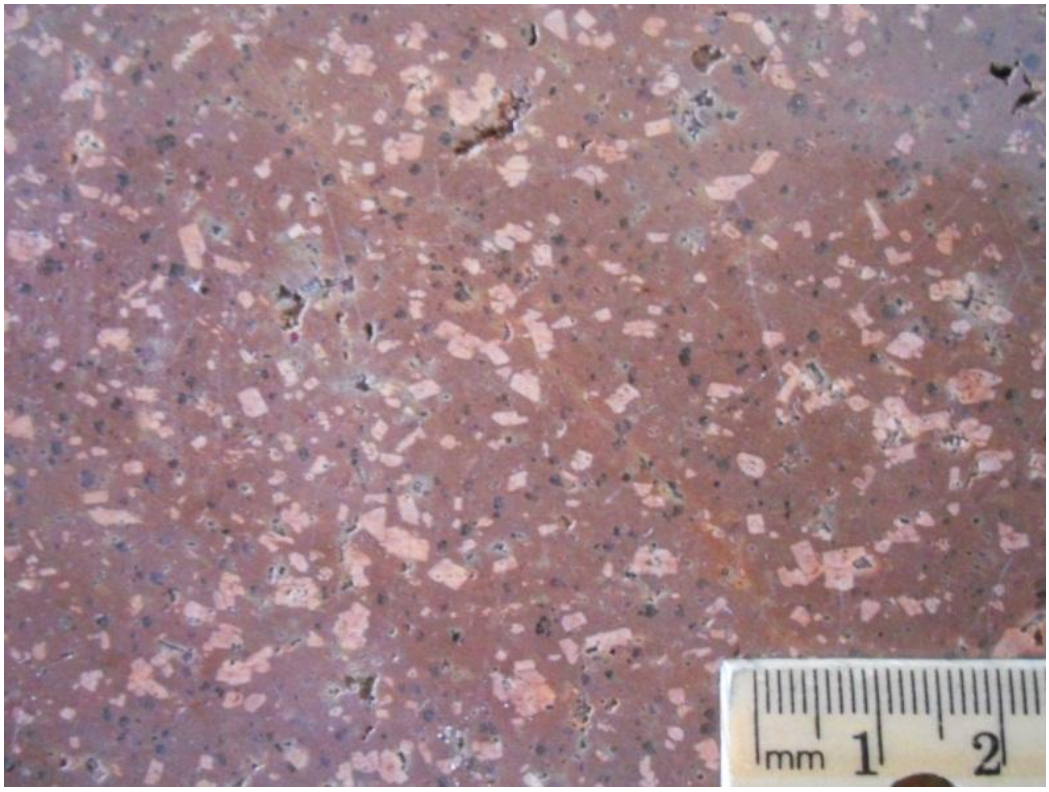

Figure 3.1. Sawn Rock Slab Showing Porphyritic Texture of the Rhyolite Dike With Salmon Colored Alkali Feldspar Phenocrysts, Grey Quartz Phenocrysts, and Open Void Spaces in a Very Fine-Grained Red Matrix of Feldspar and Quartz.

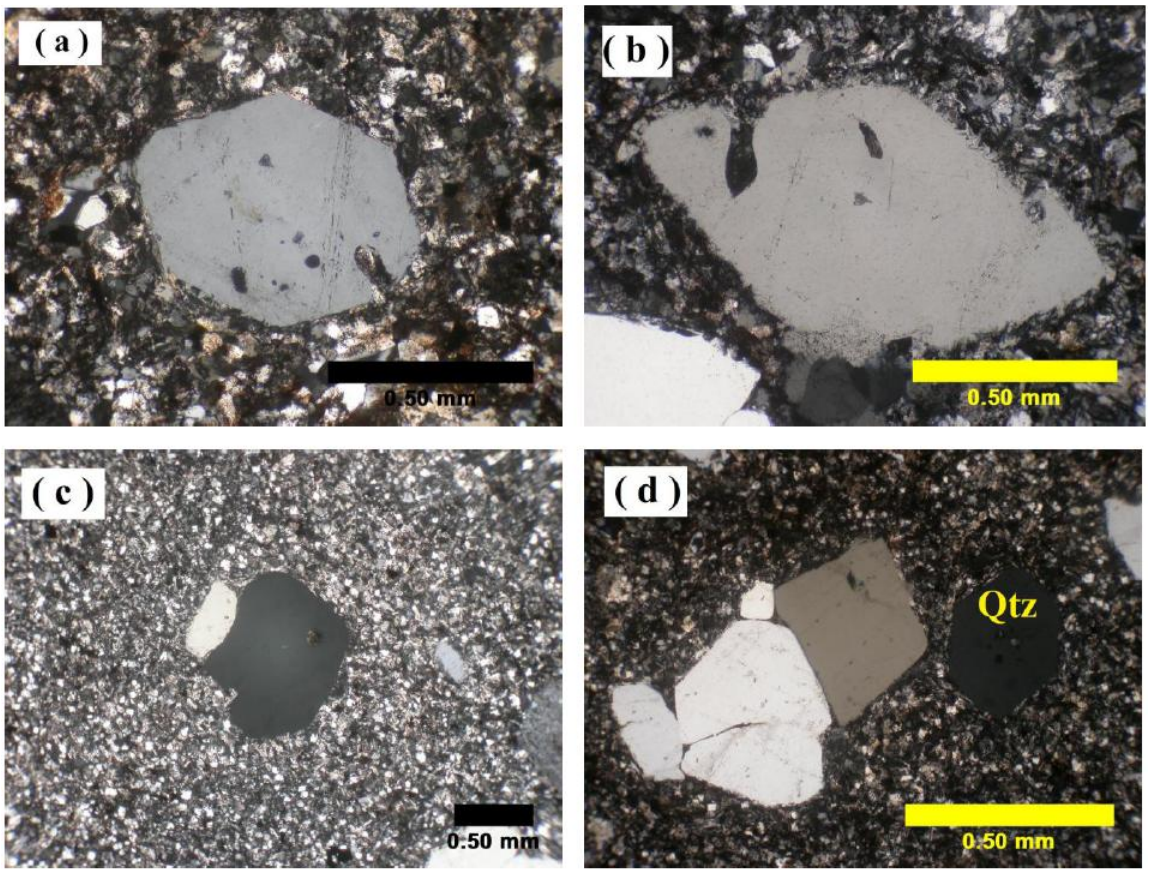

Figure 3.2. Cross-Polarized Photomicrographs of Quartz Phenocrysts. (a-b) Euhedral to subhedral quartz phenocrysts with clear traces of resorption. (c) Subhedral quartz phenocryst with evidence of melt inclusion. (d) The quartz crystal (qtz) is a rare euhedral hexagonal crystal with no obvious evidence of resorption.

3.3. QUARTZ MORPHOLOGY

Quartz phenocrysts in the rhyolite dike exhibit different morphologies. In transmitted polarizing microscopy, subhedral to anhedral quartz crystals occur both as individual crystals and as clustered phenocrysts or "glomerocrysts" (Figs 3.2, 3.3, 3.4). Euhedral quartz crystals are rare in the rhyolite dike (Fig. 3.2d). Quartz phenocrysts typically exhibit irregular outlines and embayed margins (Fig. 3.3c) even if they still

preserve a nearly euhedral form (Fig. 3.2 a, b). Quartz crystals have been observed as inclusions in alkali feldspar crystals, but such inclusions are extremely rare (Table 3.1). The boundary layer melts that formed around the crystals during minerals dissolution are finer than the matrix and it is saturated in SiO_2 (Fig. 3.4).

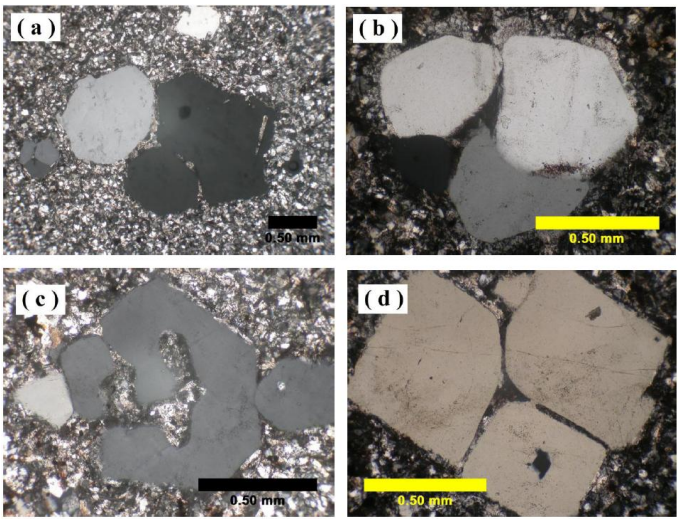

Figure 3.3. Cross-Polarized Photomicrographs of Quartz Glomerocrysts in Rhyolite Dike. Glomerocrysts are comprised of anhedral (a, b) to subhedral (c, d) quartz phenocrysts with irregular embayed edges that may exhibit quartz-quartz contacts or be separated by a thin domain of groundmass.

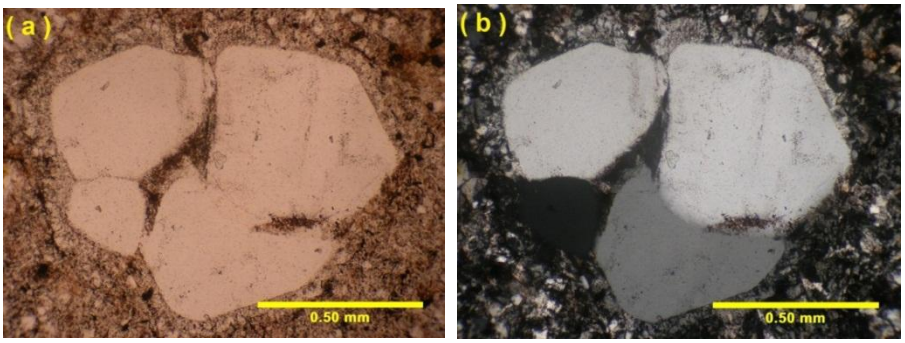

Figure 3.4. Plane-Polarized Photomicrograph and Cross-Polarized Photomicrograph Show the Boundary Layer Around the Quartz Phenocrysts.

Table 3.1 presents the main petrographic observations for quartz phenocrysts from the rhyolite dike, including the slide number and circle number which provide the location of the phenocrysts. Quartz phenocrysts exhibit a diverse variety of textures, sizes and shapes as well as the potential effects of resorption.

Table 3.1. Characteristic Features for Quartz Phenocryst in Rhyolite Dike.

Slide Number	Circle Number	Phenocryst Type	Description	Photomicrograph
JH – 2 – 04c	Circle# 1	Clustered phenocryst	Phenocryst clustered anhedral quartz. Two crystals were cut perpendicular to C axis. Some evidence of resorption found	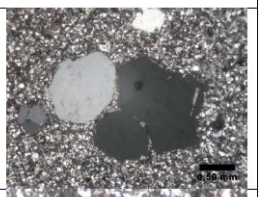
JH – 2 – 04c	Circle# 4	Quartz inside alkali-feldspar	A good example of a quartz crystal located inside a k-feldspar crystal. This may represent an example of the early growth of quartz.	
JH – 2 – 04d	Circle# 1	Clustered phenocryst	An example of a subhedral to anhedral quartz glonerocryst. Some crystals are perpendicular sections to C axis and others are oblique.	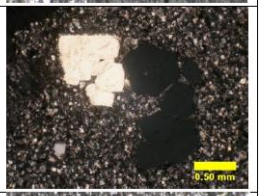
JH – 2 – 04d	Circle# 2	Individual phenocryst	An example of a subhedral, perpendicular section to C axis. It is resorbed quartz phenocryst with evidence of inclusion.	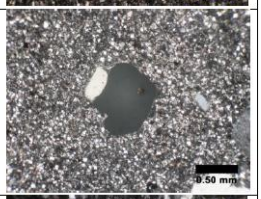
SJ – 1 – e	Circle# 2	Individual phenocryst	Resorbed individual quartz phenocryst with oblique section to C axis.	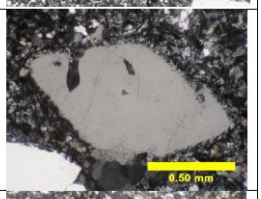
SJ – 2 – b	Circle# 2	Individual phenocryst	Resorbed hexagonal quartz phenocryst with perpendicular section to C axis of the crystal.	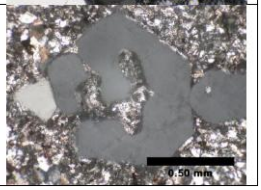

Table 3.1. Characteristic Features for Quartz Phenocryst in Rhyolite Dike (CONT.).

SJ – 3 – a	Circle# 1	Individual phenocryst	Example of hexagonal quartz (Qtz). It was cut perpendicular to C axis.	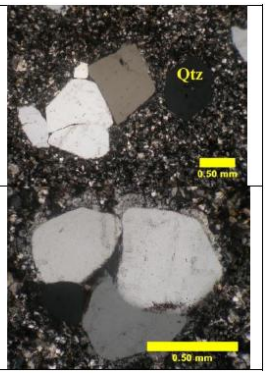
SJ – 3 –a	Circle# 2	Clustered phenocryst	Example of resorbed clustered quartz phenocryst. Good evidence of resorption is around the phenocryst.	

3.4. CATHODOLUMINESCENCE (CL)

CL images demonstrate that the quartz phenocrysts preserve a detailed record of well preserved and delicate internal compositional zonation not imaged by the petrographic microscope (Fig 3.5). The compositional zonation in the quartz crystals can be considered an internal stratigraphy that preserves a record of changing conditions in the melt during the crystal growth history of individual phenocrysts. The slight variation in the trace element composition of the quartz phenocrysts during crystallization will depend on the composition of the melt and changes in pressure and temperature at the time and location of crystal growth (Kirkpatrick, 1975). Thin multiple oscillatory zonations record local near surface fluctuations in trace element concentrations at the crystal-melt interface as a result of feedback between crystal growth rates and diffusion rates of trace elements in the melt. Abrupt changes in CL intensity may reflect more extensive regional changes in melt temperature and or melt composition, possibly as a

result of magma mixing events. In addition, truncation of internal zonation of the crystals is similar to unconformities in that they record removal of material during periods of crystal dissolution (Watt et al. 1997; Muller et al. 2010).

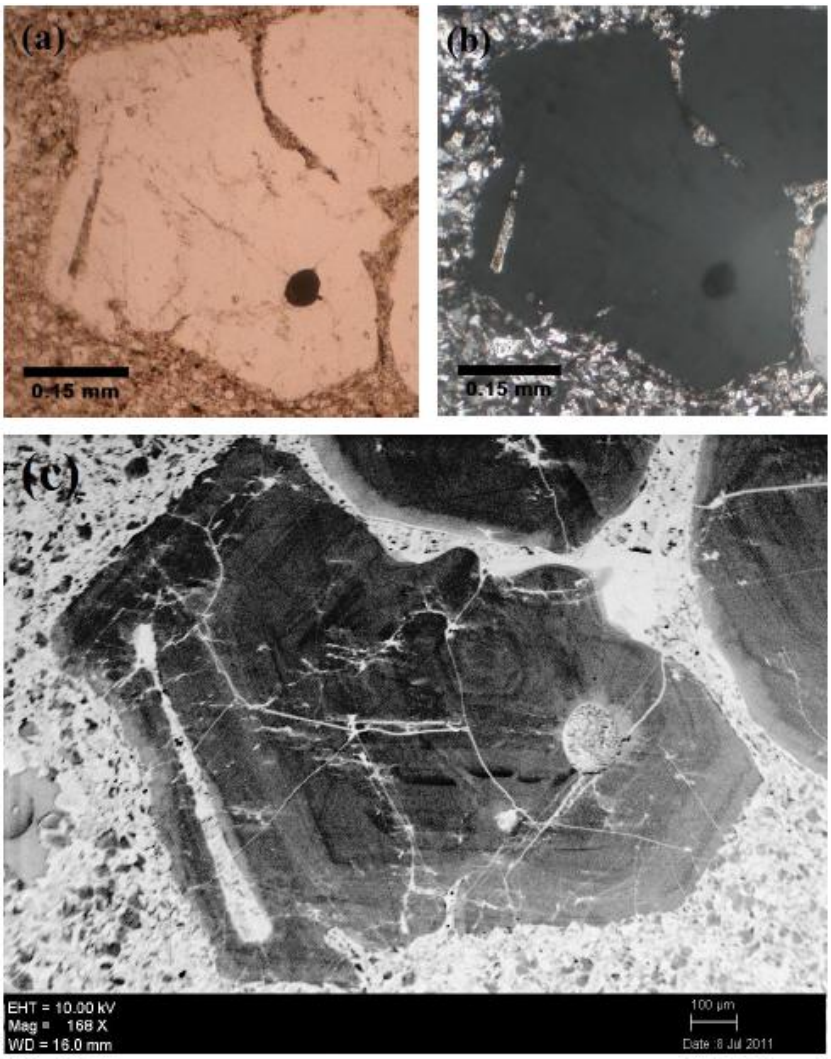

Figure 3.5. (a) and (b) Are Plane Polarized and Cross Polarized Photomicrographs of a Quartz Phenocryst Respectively Showing a Uniform Internal Appearance of the Phenocryst. (c) Cathodoluminescence photomicrograph of the same quartz phenocryst illustrates designed internal fine scale oscillatory zonation, well developed bright zones, and clear and abrupt truncation of internal zonation along the edge of the phenocryst.

The CL intensity in quartz is related to the Ti concentration (Wark and Spear, 2005), and CL images of quartz from igneous rocks have successfully been used to constrain the crystallization history of magmas similar to the way in which compositional zoning in plagicoclase (visible in petrographic microscopes) has been used (Wiebe et al. 2007). The Ti content of quartz has also been shown to be a function of temperature, with higher Ti contents reflecting crystallization of quartz from higher temperature systems (Wark and Watson, 2006) as well as the activity of Ti in the melt and pressure. Changes in CL intensity may also be affected by radiation damage, lattice defects and effects that occur at grain boundaries (Walderhaug and Rykkje, 2000). The CL zoning discussed below focuses on regions in the grains that best preserve primary magmatic zoning (the focus of this study), other areas that may reflect subsolidus overprinting or edge effects are not discussed. Zones that are brighter towards the core of the crystal (i.e., higher Ti and presumably higher temperature) and become darker towards the margin (i.e., lower Ti and presumably lower temperature) are termed "normal". Zones that are darker towards the core of the crystal and gradually become brighter towards the margin are termed "reversed." Domains comprised of fine scale minor concentric variations in intensity are termed "oscillatory".

All the quartz phenocryst CL images record internal growth zonation commonly exhibiting oscillatory zoning, normal zoning and reverse zoning within the same quartz phenocryst (Figs. 3.1, 3.2, 3.3). Domains characterized by oscillatory growth zoning commonly exhibit euhedral crystal forms that record the former margin of the crystal, demonstrating the zonation is magmatic (Fig.3.6c). These zones commonly exhibit overall normal zonation (Fig. 3.5c). Reverse zonation is also observed where bright CL

zones form on the outside edge of the darker CL domains (Fig. 3.5c). The contacts are commonly sharp and irregular and the older growth zoning can be truncated along an internal resorption surface followed by renewed periods of oscillatory growth zoning (Fig. 3.6c). Important to this study is that all crystals show abrupt termination, commonly at high angles, of the oscillatory growth zoning along the outermost surface (i.e., edge) of the phenocryst. In addition, several thin brittle fractures cross-cut phenocrysts but do not appear to offset the compositional zonation, indicating the thin fractures postdate crystallization and record a later brittle event (Fig. 3.7).

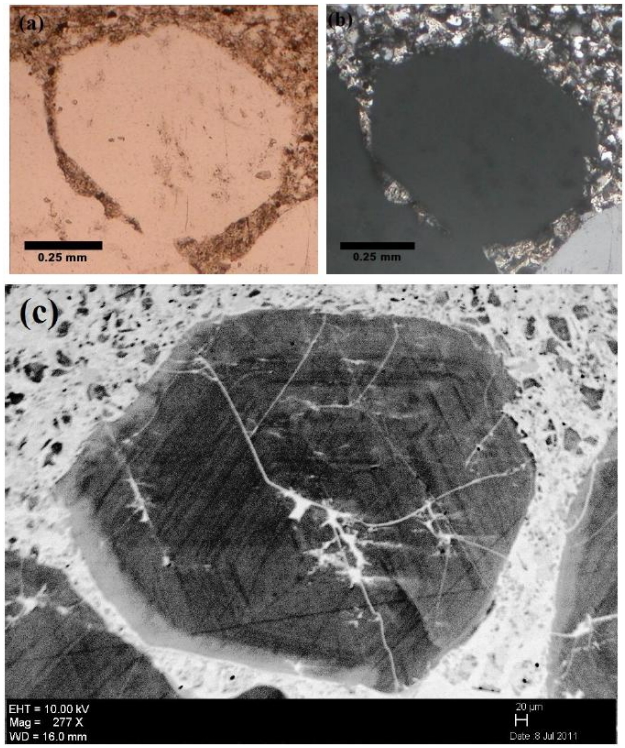

Figure 3.6. (a) and (b) Are Plane Polarized and Cross Polarized Photomicrographs of Quartz Phenocryst. (c) Cthodoluminescence photomicrograph.

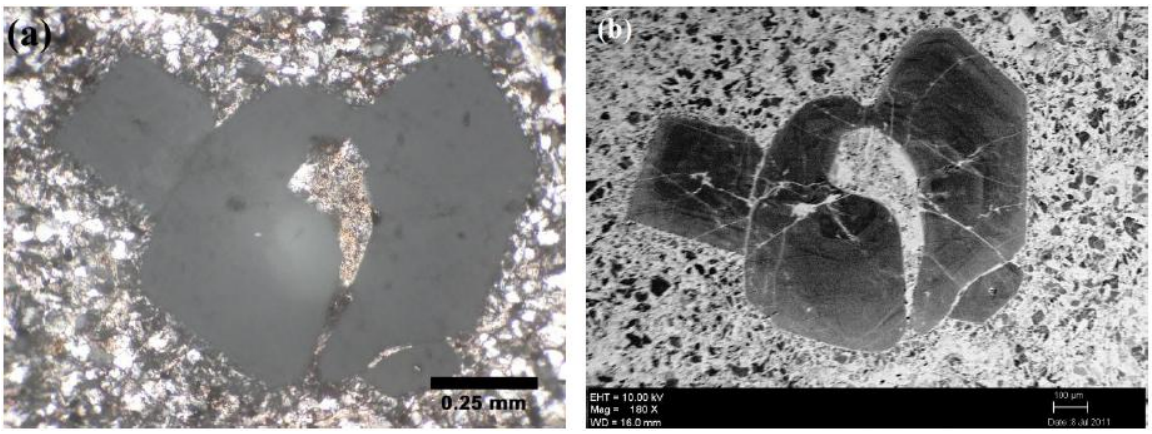

Figure 3.7. Resorbed and Embayed Quartz Crystal. (a) Cross polarized photomicrograph and (b) cathodoluminescence photomicrograph.

Resorbed and embayed (Fig. 3.2) quartz crystals and dissolution surfaces are found in the crystals but are prominent at the core and near the rim. Resorption surfaces are typically rounded dissolution patterns (carves texture)and are commonly associated with bright-CL zones. Figure 3.2 shows a good example of a resorbed and embayed quartz crystal; the color becomes brighter from core to rims.

Juxtaposed quartz phenocrysts in glomerocrysts exhibit internal compositional zonation that is abruptly truncated at the edge of the pheonocryst as revealed by CL (Figs. 3.1, 3.2, 3.3). Evidence for a shared compositional zonation, indicating a period of common growth, between glomerocryst grains has been not observed in the rhyolite dike.

4. INTERPRETATION AND DISCUSSION

The texture of many igneous rocks depends on the phenocrysts (Jerram et al. 2003). In the igneous rocks, phenocrysts occur as both individual crystals and as a mixture of individual and clustered phenocrysts (Fig. 4.1). Quartz glomerocrysts, clusters of quartz comprised of typically two to six individual quartz phenocrysts, are a distinctive petrographic feature of the rhyolite dike in Medicine Park, Oklahoma. Similar monomineralic glomerocrysts are a common feature in the granites as well, including members of the Wichita Granite Group. Two models have been proposed to explain the origin of these monomineralic clusters in igneous rocks: 1) synneusis, the drifting together and attachment of crystals, suspended in a melt, along similar prominent crystal faces during crystallization (Vogt, 1921; Vance 1969) and 2) resorption aggregation where dissolving crystals that come into close proximity become attached due to crystallization of their overlapping boundary layer melts that develop adjacent to the dissolving crystals (Hogan, 1993) (Fig. 4.2). Distinguishing between these two processes has relied on the morphology of the attached crystals. Glomerocrysts that are comprised of crystals that can be shown to share prominent planar crystallographic faces have been attributed to forming during crystallization as the result of synneusis (Schwindlinger and Anderson, 1989). In contrast, glomerocrysts comprised of clusters of anhedral rather than euhedral crystals have been suggested to have formed while dissolving in the melt as a result of resorption aggregation (Hogan, 1993).

The external morphology of the crystals is a non-unique test to distinguish between the two processes that may lead to glomerocryst formation. The external morphology is controlled by the growth rate and element diffusion in the melt

(Kirkpatrick, 1975) both of which vary with undercooling. The resulting textures of the igneous rocks have been shown to differ with variation in undercooling as well, where anhedral to skeletal crystals can form during crystallization large undercoolings (Swanson, 1977). Thus, it is possible that the morphology of the subhedral to embayed quartz phenocrysts observed in transmitted polarized light microscopy (Figs. 3.2 and 3.3) could be either the result of resorption or alternatively formed as a result of more rapid growth in large undercoolings. In contrast, the results of the CL investigation of quartz phenocrysts in the rhyolite dike at Medicine Park, Oklahoma unequivocally demonstrate that the internal compositional growth zoning is abruptly truncated along the external crystal surface, indicating these phenocrysts were in the process of being dissolved back into the melt at the time the glomerocrysts were being formed.

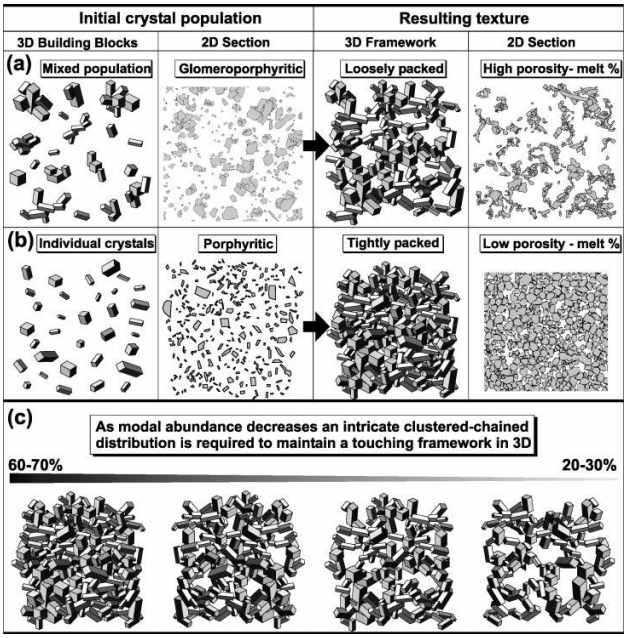

Figure 4.1. The Development of Phenocryst Population as Initial Building Blocks (Jerram et al. 2003).

The process of glomerocryst formation as a result of resorption aggregation (Hogan, 1993) requires the development of a boundary layer melt, enriched in the components of the dissolving crystal, to develop adjacent to the dissolving crystal (Fig. 4.2). This boundary-layer melt forms if the rate of crystal dissolution exceeds the rate of diffusion of these components (Kuo and Kirkpatrick 1985; Tsuchiyama and Takahashi 1985; Wark and Stimac 1990). According to Liang (1999), the resorption rates are not related to the crystal axis and the orientation of the crystals, rather the resorption rates are related to the composition of the magma at the time the crystals are dissolving. Wider boundary-layer melts can grow at high crystal dissolution rates, while the boundary-layer melt will remain thin if diffusion rates are high enough to disperse away the chemical species from the crystal-melt boundary (Watson, 1982). Thin (10μm) zones of very fine grained quartz and feldspar that occur along the margins of resorbed quartz phenocrysts may be manifestations of former boundary layer melts that developed during quartz dissolution in the rhyolite dike. Subsequent to initiation of crystal dissolution, two or more resorbed crystals must come in close enough proximity their boundary layer melts to overlap and create an intervening zone of component enrichment that crystallizes to form a shared permanent contact and develop a glomerocryst (Fig. 4.2). The abundance of quartz crystals in the magma at the time of resorption increases the potential for the crystals to come into close proximity allowing boundary layer melts to overlap and lead to glomerocryst formation.

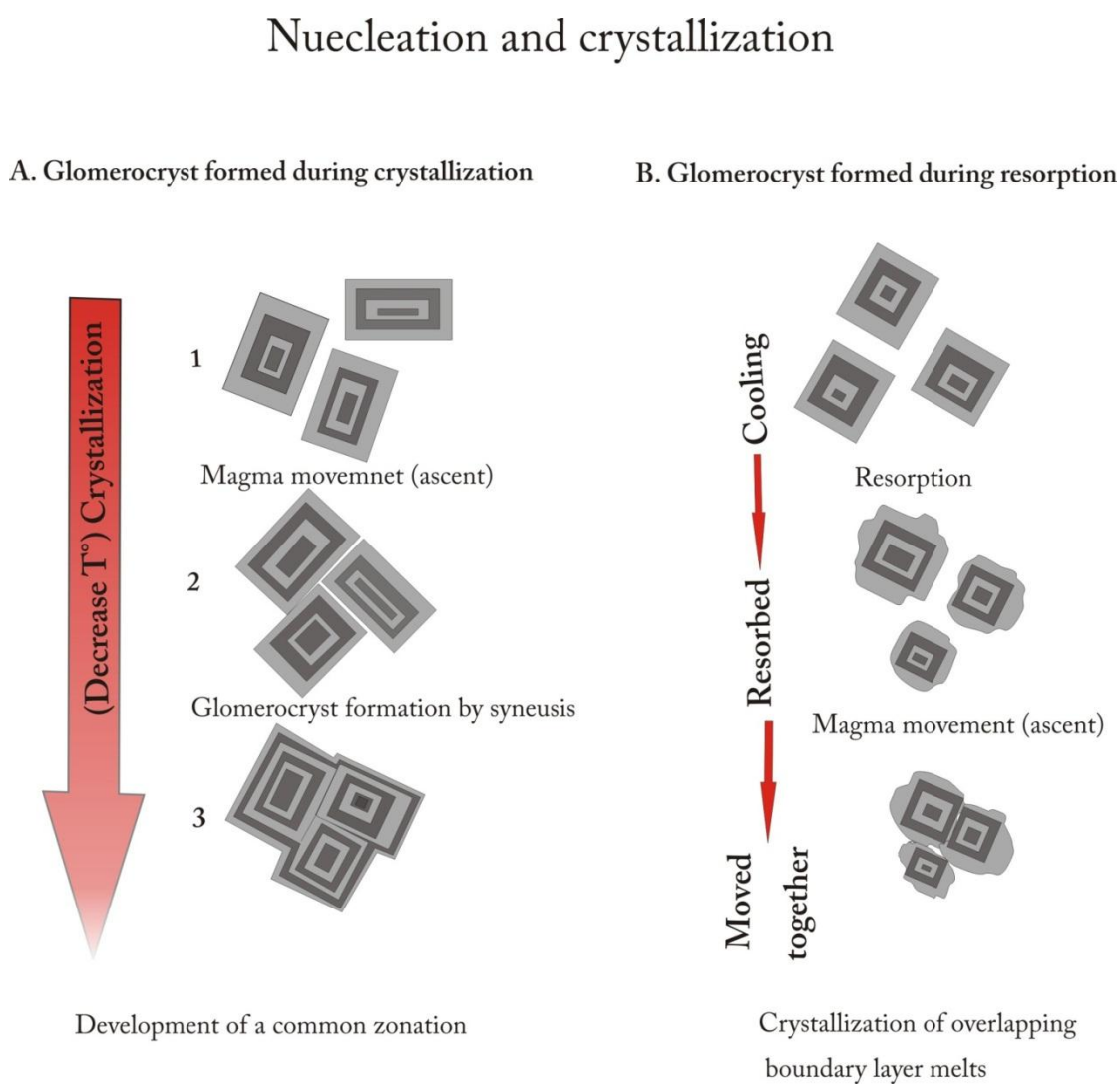

Figure 4.2. Schematic Model Illustrates Formation of Glomerocrysts During Syneusis and Resoprtion.

4.1. RESORPTION AND GLOMEROCRYST FORMATION

The resorption of the minerals during cooling of a “closed system” magma chamber may take place through changes in melt composition (e.g., peritectic crystallization), circulation of crystals from regions in the magma chamber that exhibit

large enough differences in temperature or aH_2O to destabilize the mineral assemblage, decreases in pressure during ascent, or a combination of these possibilities. In open system magmas, resorption may record an increase in intensive parameters such as melt temperature, aH_2O or a change in melt composition as the result of the influx of a significantly hotter or compositionally distinct magma into the crystallizing chamber.

4.2. MAGMA REPLENISHMENT

The rhyolite dike at Medicine Park is interpreted to have crystallized as a relatively closed system, as direct evidence for involvement of a mafic magma, such as the presence of mafic enclaves or ocelli, were not observed (Price, 1998). The scenario of mafic magma replenishment is unlikely to be responsible for forming the exterior resorbed surface on the quartz crystals. However, it is possible that some of the reverse zonation and internal resorbed surfaces within quartz penocrysts imaged by CL (Fig. 4.3) may be the result of an increase in magma temperature as the result of influx of a hotter magma of unknown composition or of circulation of crystals from cooler regions to hotter regions in the magma chamber.

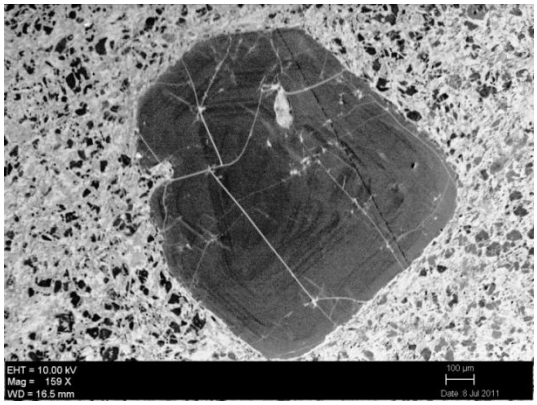

Figure 4.3. CL Image Shows Reverse Zonation and Internal Resorbed Surfaces within a Quartz Phenocryst.

4.3. DECOMPRESSION

In felsic magmas, quartz crystals have the greatest potential to undergo resorption as a result of decompression during magma ascent (Nekvasil, 1991). The magma that eventually formed the rhyolite dike initially began crystallization in a deeper level storage chamber where quartz and alkali feldspar crystals were crystallizing simultaneously from the melt as individual euhedral crystals (Fig. 4.4). Using phase equilibria and amphibole geobarometry Hogan and Gilbert (1995) proposed that the Mount Scott Granite also began crystallization in a storage chamber which developed along a crustal magma trap at a depth of ~8.0 km or 200 MPa before ascending to be emplaced beneath the volcanic cover. This depth for the rhyolite dike storage chamber will be adopted here for purposes of discussion. During ascent of the magma from the storage chamber at pressure 200MPa to the emplacement level at pressure 50MPa, the position of the quartz-feldspar cotectic in the system SiO_2-$NaAlSi_3O_8$-$KAlSiO_8$-H_2O shifts towards the SiO_2 component, expanding the stability field for feldspar and decreasing the stability field for quartz. This shift of the cotectic with decreasing pressure during ascent places the melt composition entirely in the stability field for feldspar, resulting in resorption of quartz phenocrysts (Fig. 4.4). The melt composition then corresponds with the cotectic at the emplacement level pressure which approximately equal 50MPa (Hogan and O'Donnell, 2008).

4.4. FORMATION OF GLOMEROCRYSTS

During magma ascent, quartz crystals were undergoing resorption in response to decompression. At this time boundary layer melts would develop around the crystals. During ascent the movement of the magma would provide the motion necessary to bring

dissolving quartz crystals into close proximity of other dissolving quartz crystals (Fig. 4.4). Overlap of the boundary layer melts, which have elevated abundances of the dissolving mineral components (i.e., SiO_2) result in crystallization of the quartz from this overlap zone leading to glomerocryst formation (Hogan, 1993). The rhyolite magma then reaches the emplacement level where the melt thermally quenches, locking in the porphyritic, glomerocrystic texture of the intrusive dike that leaving appearance of a volcanic rhyolite (Fig. 4.4). The composition of the matrix is a proxy for the composition of the quenched melt and corresponds with the 50 MPa cotectic consistent with an epizonal to subvolcanic level for emplacement (Hogan and O'Donnell, 2008).

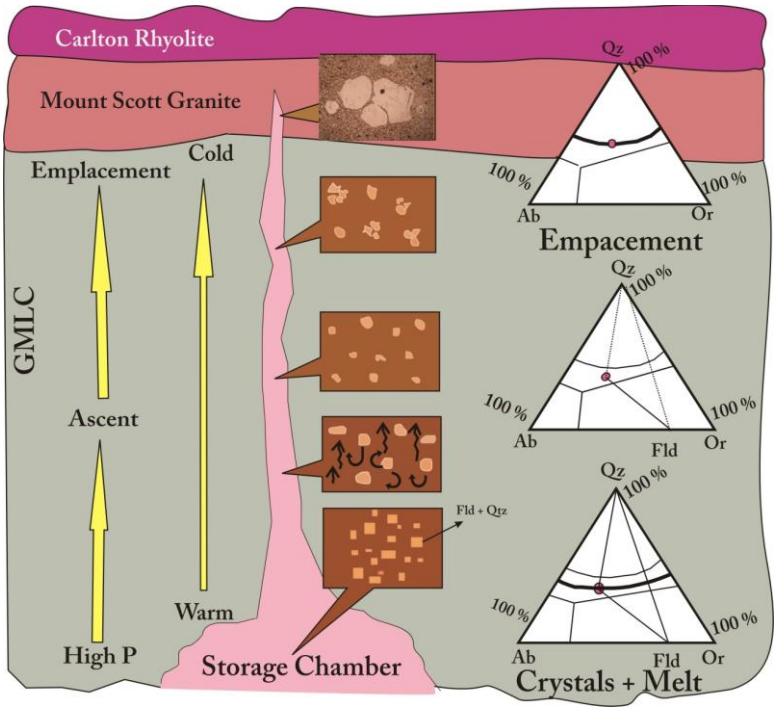

Figure 4.4. Schematic Model Illustrates the History of Quartz Crystals in the Rhyolite Dike from the Storage Chamber to the Emplacement Level.

5. CONCLUSION

A detailed petrographic and cathodoluninescence investigation of quartz glomerocrysts from the rhyolite dike at Medicine Park demonstrated that internal compositional zonation which developed in quartz phenocrysts during crystallization is abruptly truncated along the irregular embayed external surfaces of the quartz phenocrysts, readily observed using a petrographic microscope. The results of the CL study then unequivocally link the anhedral and embayed morphology of the quartz phenocrysts to the process of resorption, where material was being removed from the surface of quartz crystals as they were being dissolved back into the melt. The driving force for resorption of quartz is attributed to the retreat of the quartz-feldspar cotectic in the system SiO_2-$NaAlSi_3O_8$-$KAlSiO_8$-H_2O towards the SiO_2 component, which expands the stability field for feldspar and decreases the stability field for quartz in the presence of melt, with decreasing pressure during magma ascent. During ascent, the dissolving quartz crystals are brought into close contact by movement of the magma, leading to overlap of their boundary layer melts and the formation of quartz glomerocrysts by resorption aggregation (Hogan, 1993). The common occurrence of quartz glomerocrysts in granites and other igneous rocks suggests that this texture may have formed by a similar process, thus providing evidence for movement of the magma from the source region at deeper levels in the crust to the shallower depths where the magma is emplaced.

APPENDIX A

MICROSCOPIC PHOTOMICROGRAPHS

Criteria for classifying samples:

This classification depends on the type of the quartz phenocryst. The quartz phenocrysts are either individual crystals or glomerocrysts. Both of these kinds have subcategories as shown below.

1- Individual quartz crystal phenocrysts.

a- euhedral quartz crystal.

b- subhedral quartz crystal.

c- anhedral quartz crystal.

d- resorbed quartz crystal.

e- unresorbed quartz crystal.

f- section close to perpendicular to C axis of the crystal.

g- section oblique to the C axis of the crystal.

These subcategories are used to describe glamerocrysts phenocrests as well.

2- Clustered quartz crystals phenocrysts.

a- Two crystals.

b- Three crystals.

c- Four or more crystals.

Note: the micro scales in all following photos are 0.5 mm

JH – 2 – 04c:

(Circle# 1):

This is a clustered anhedral quartz phenocryst (Fig. 1). Two crystals were cut perpendicular to C axis. Some evidence of resorption is found.

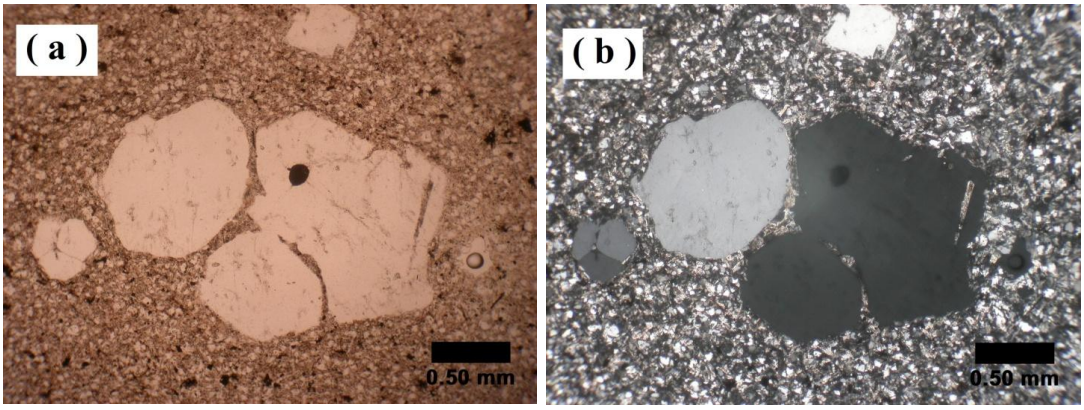

Figure 1: (a) plane-polarized photomicrograph and (b) is cross-polarized photomicrograph.

(Circle# 2):

Figure 2 shows subhedral quartz glomerocryst, resorbed, clustered and perpendicular to C axis.

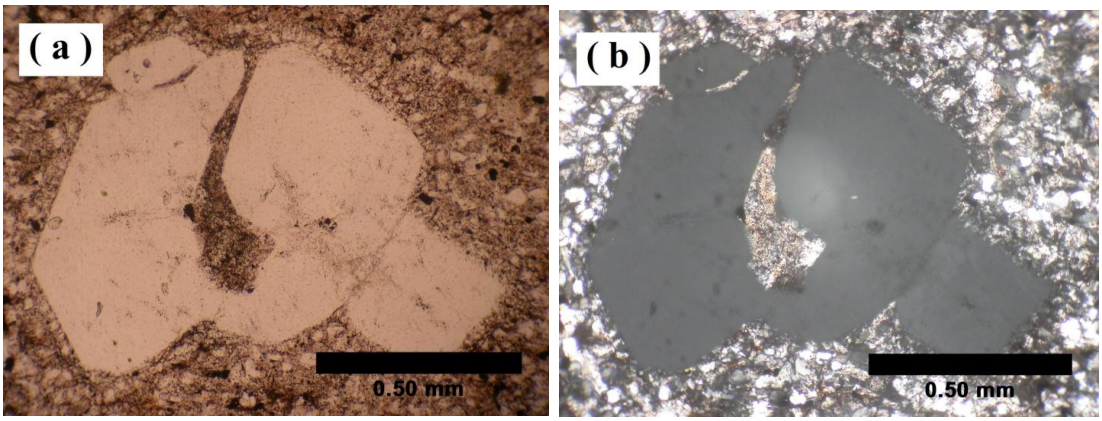

Figure 2: (a) plane-polarized photo micrograph and (b) cross-polarized photomicrograph.

(Circle# 3):

Figure 3 is an example of small euhedral quartz crystals with perpendicular section to C axis.

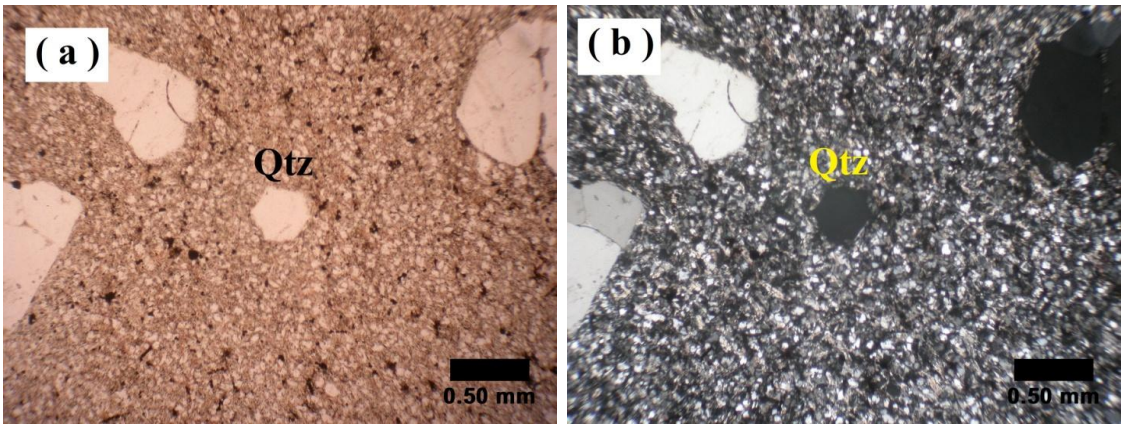

Figure 3: (a) plane-polarized photomicrograph and (b) cross-polarized photomicrograph.

(Circle# 4):

This is a good example of a quartz crystal located inside a k-feldspar crystal (Fig. 4). This may represent an example of the early growth of quartz. Because it is sequestered in feldspar it may preserve a temperature indicative of the beginning of quartz crystallization.

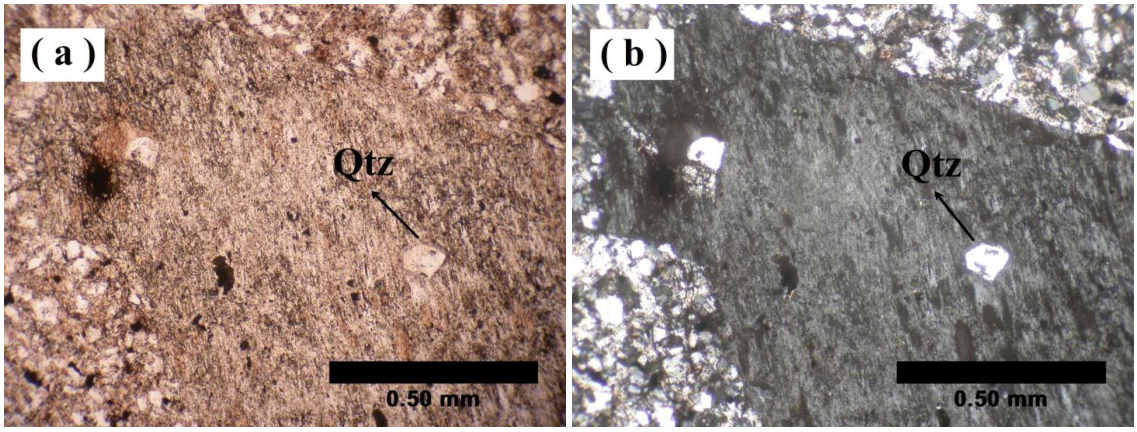

Figure 4: (a) plane-polarized photomicrograph and (b) cross-polarized photomicrograph.

(Circle# 5):

This is an example of a large subhedral quartz crystal with oblique section to C axis section (Fig. 5).

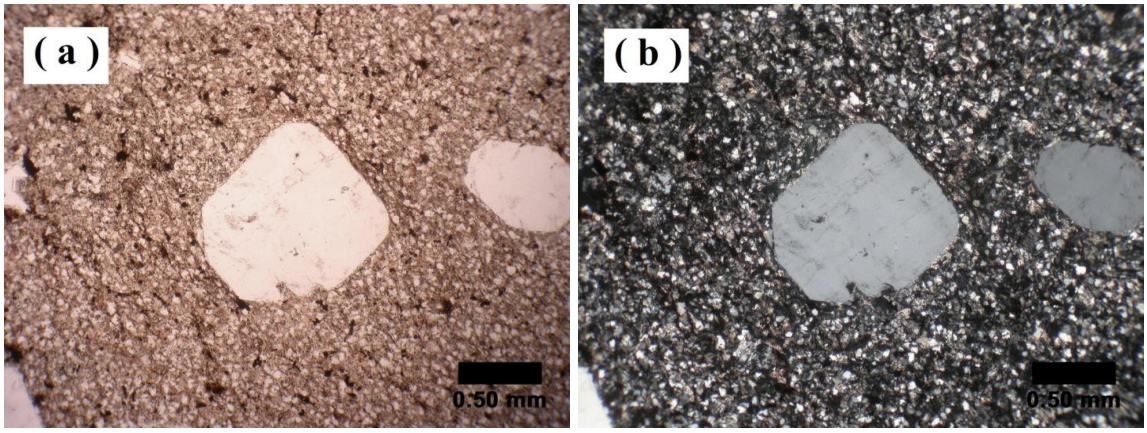

Figure 5: (a) plane-polarized photomicrograph and (b) cross-polarized photomicrograph.

JH – 2 – 04d:

(Circle# 1):

This is an example of a subhedral to anhedral quartz glomerocryst (fig.6). Some quartz crystals were cut perpendicular to the C axis and others are oblique.

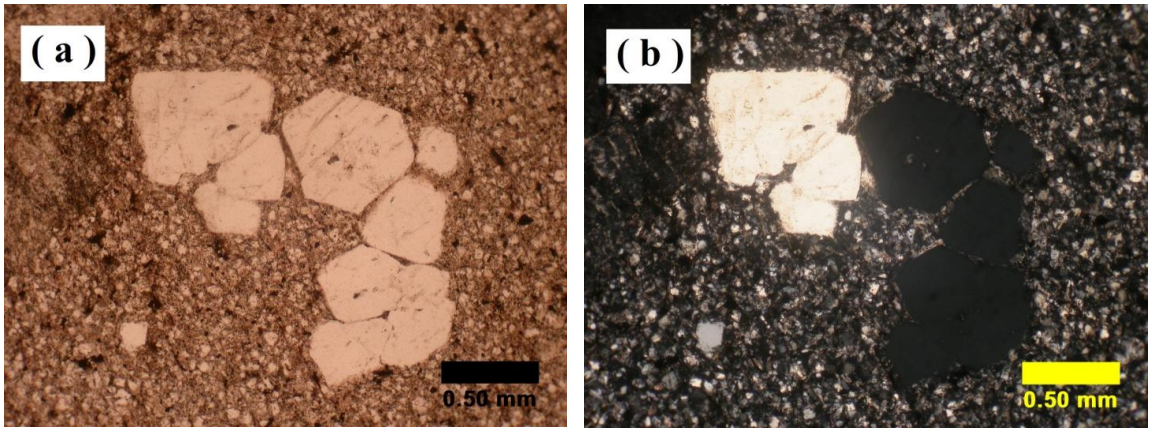

Figure 6: (a) plane-polarized photomicrograph and (b) cross-polarized photo micrograph.

(Circle# 2):

This is a good example of a subhedral, perpendicular section to the C axis and a resorbed individual quartz phenocryst with evidence of inclusion (fig.7).

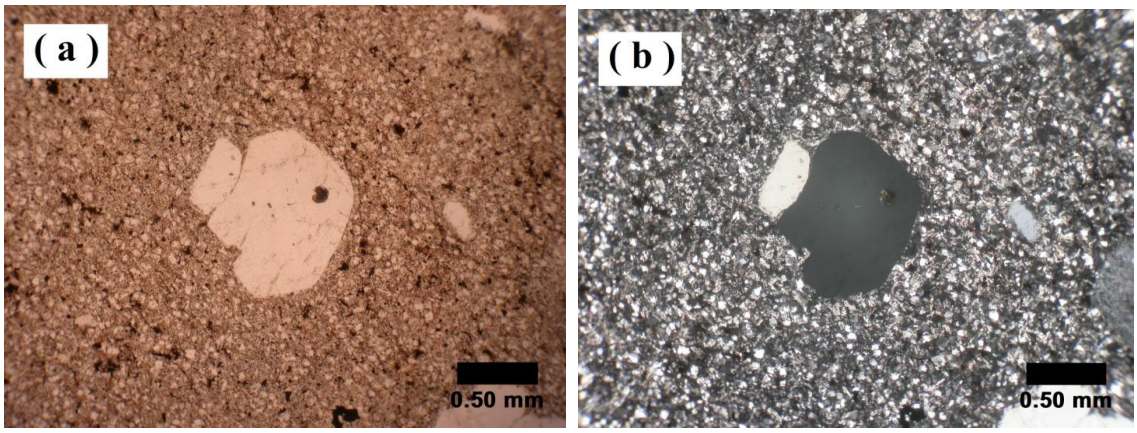

Figure 7: (a) plane-polarized photomicrograph and (b) cross-polarized photomicrograph.

(Circle# 3):

Figure 8 displays a hexagonal individual quartz phenocryst, perpendicular to the C axis of the crystal.

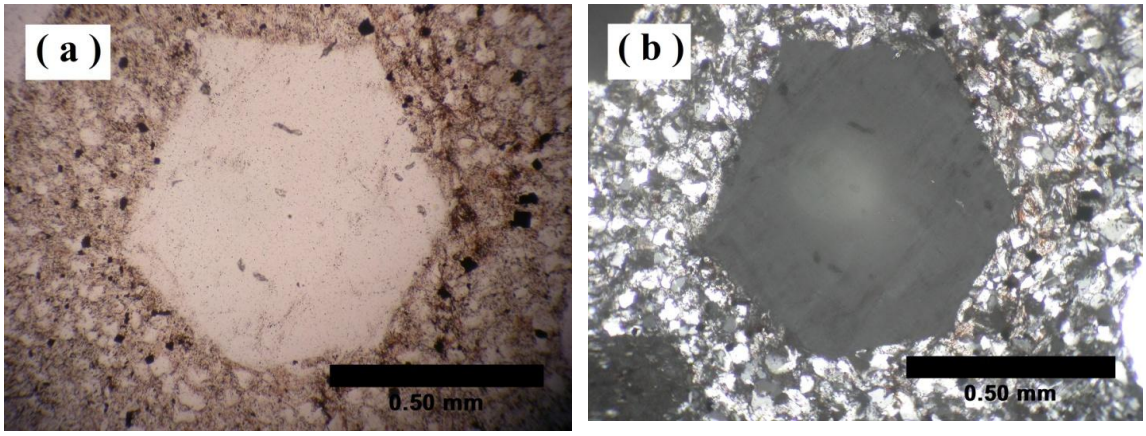

Figure 8: (a) plane-polarized photomicrograph and (b) cross-polarized photo micrograph.

(Circle# 4):

Figure 9 displays an example of a small quartz euhedral phenocryst with a perpendicular section to the C axis.

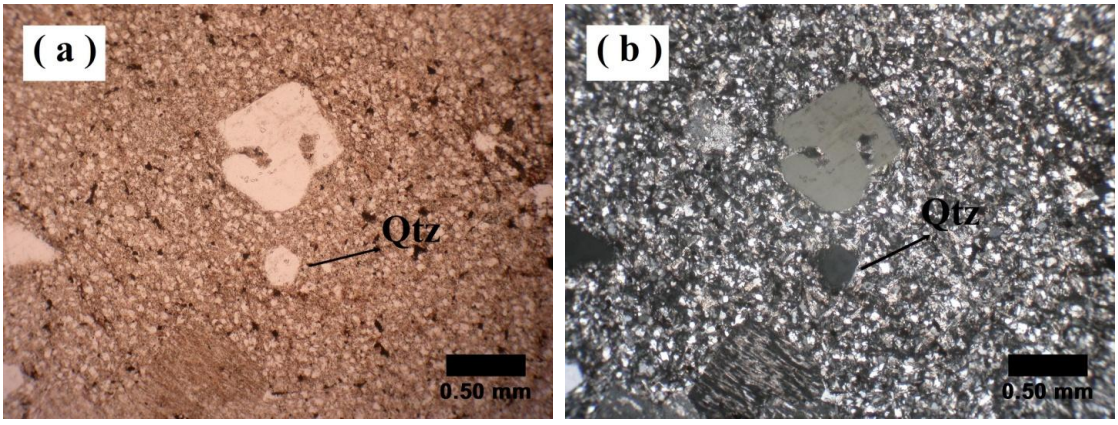

Figure 9: (a) plane-polarized photomicrograph and (b) cross-polarized photomicrograph.

(Circle# 5):

This is an example of a large quartz subhedral crystal (fig. 10).

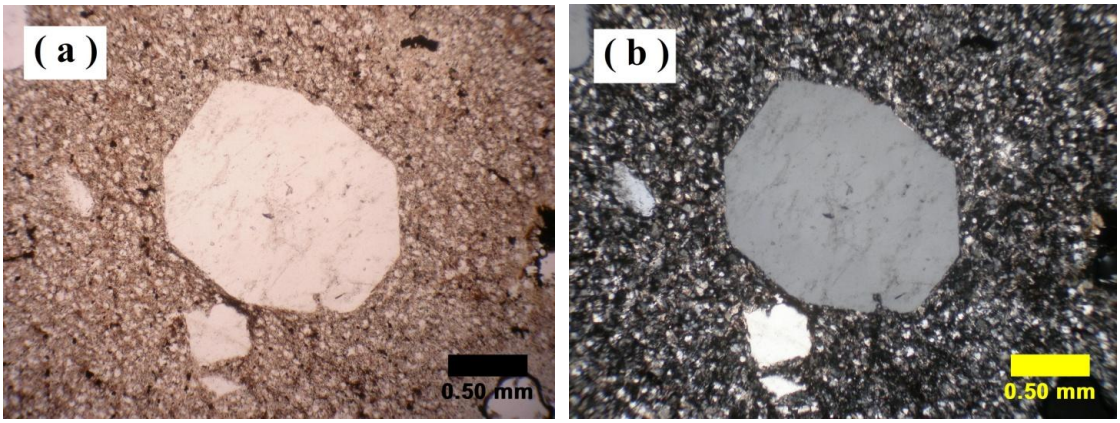

Figure 10: (a) plane-polarized photomicrograph and (b) cross-polarized photomicrograph.

(Circle# 6):

Figure 11 shows a large subhedral quartz phenocryst.

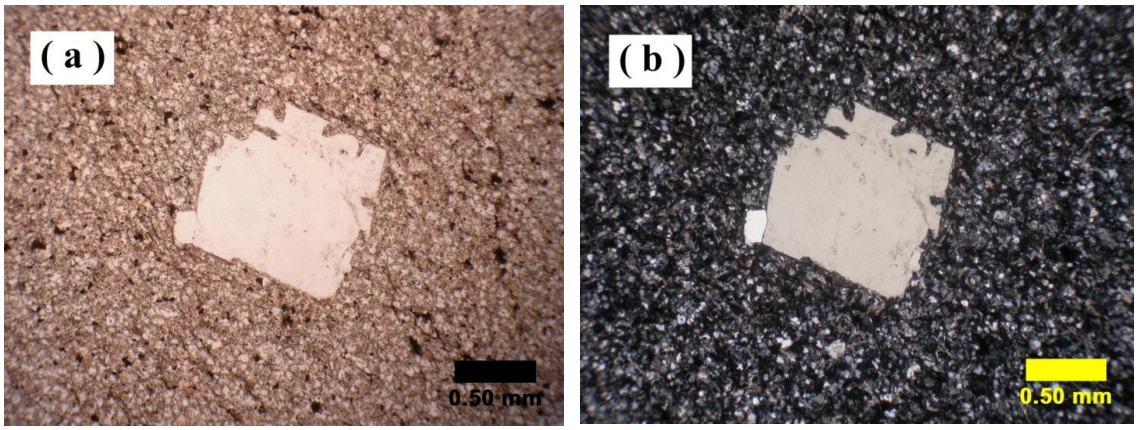

Figure 11: (a) plane-polarized photomicrograph and (b) cross-polarized photomicrograph.

SJ – 1 – e:

(Circle# 1):

This is an example of an anhedral resorbed clustered quartz phenocryst. These crystals were cut very close to the C axis (fig.12).

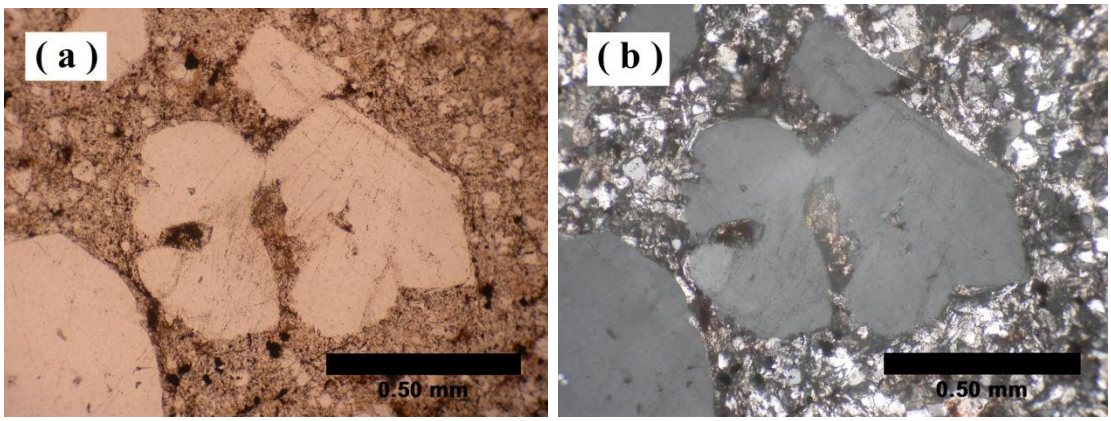

Figure 12: (a) plane-polarized photomicrograph and (b) cross-polarized photomicrograph.

(Circle# 2):

Figure13 illustrates resorbed individual quart phenocryst with an oblique section to the C axis.

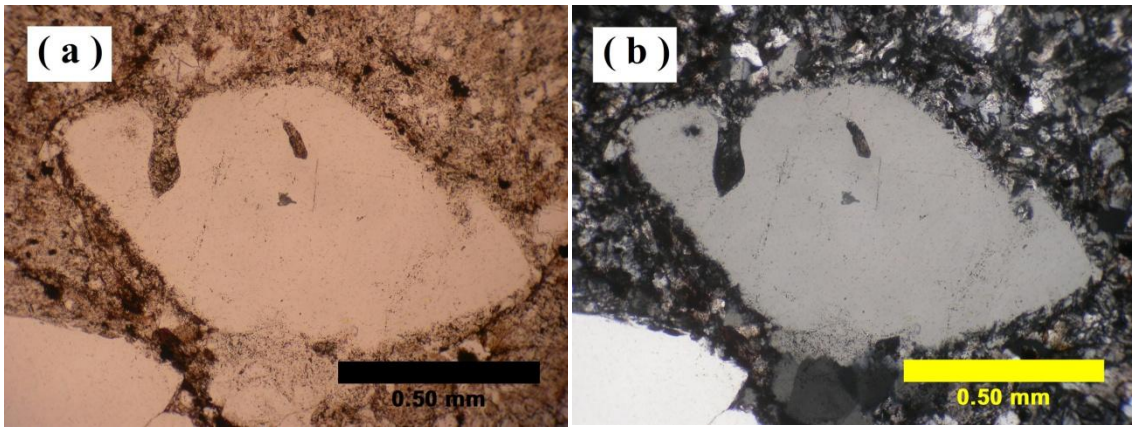

Figure 13: (a) plane-polarized photo micrograph and (b) cross-polarized photomicrograph.

(Circle# 3):

Figure 14 illustrates small subhedral to euhedral quarts phenocrysts

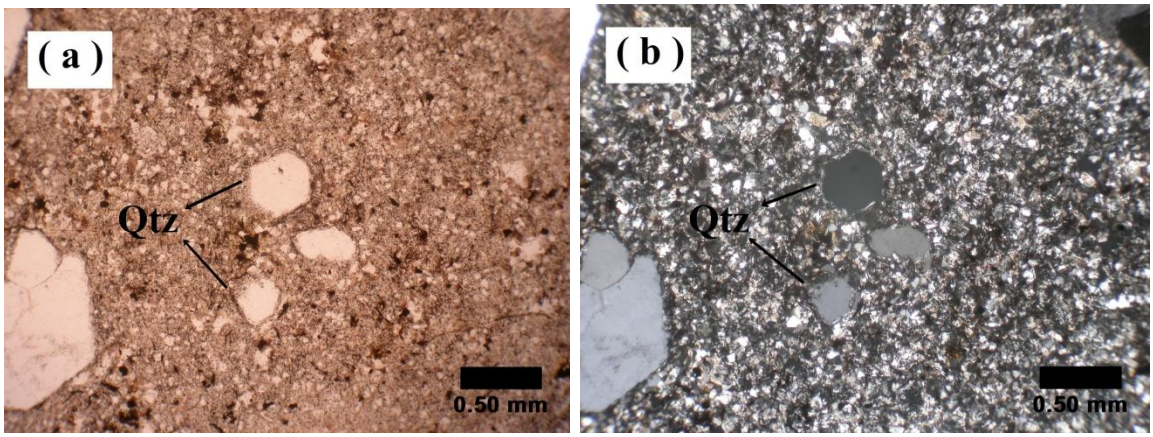

Figure 14: (a) plane-polarized photomicrograph and (b) cross-polarized photo micrograph.

(Circle# 4):

This is an example of a miarolitic cavity in this rhyolite dike. These small quartz crystals around the cavity could be crystallized as a late generation of the quartz crystallization (fig. 15).

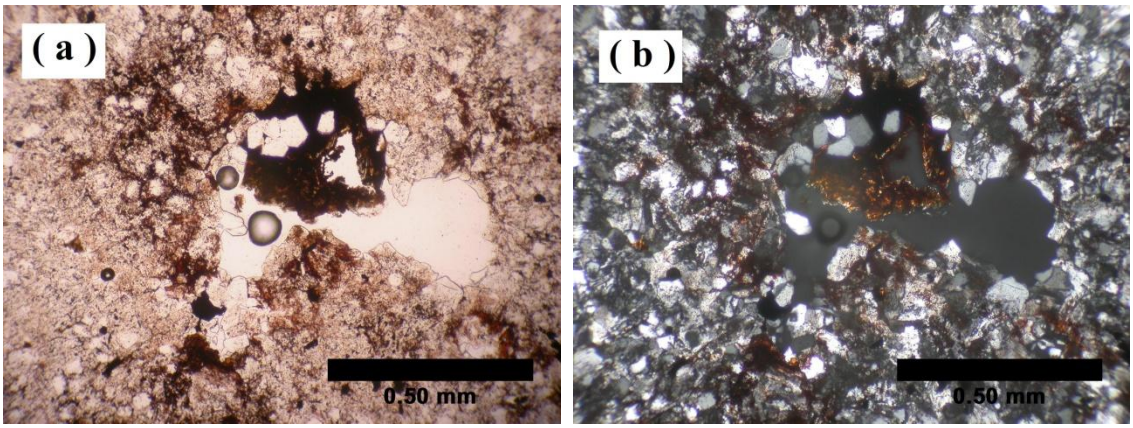

Figure 15: (a) plane-polarized photomicrograph and (b) cross-polarized photomicrograph.

(Circle# 5):

Figure 16 shows a large subhedral quartz phenocryst.

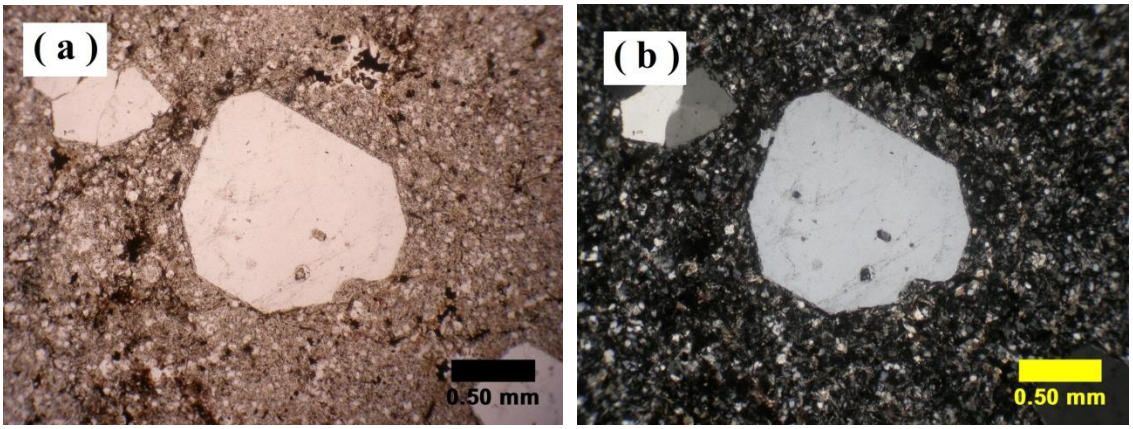

Figure 16: (a) plane-polarized photomicrograph and (b) cross-polarized photomicrograph.

SJ – 2 – b:

(Circle# 1):

This is an example of hexagonal quartz (Qtz) that was cut perpendicular to the C axsis (fig. 17).

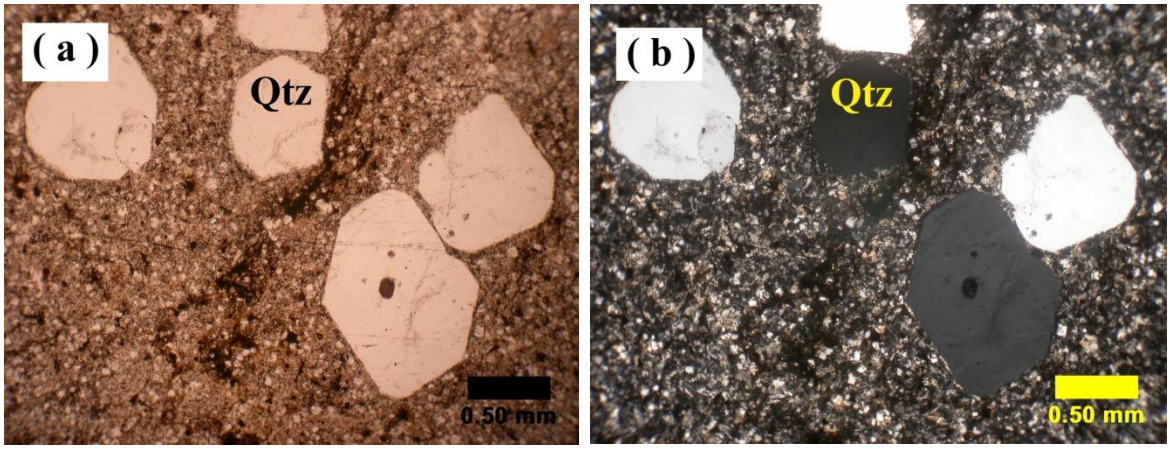

Figure 17: (a) plane-polarized photomicrograph and (b) cross-polarized photomicrograph.

(Circle# 2):

Figure 18 shows a resorbed hexagonal quartz phenocryst. It was cut perpendicular to the C axis of the crystal.

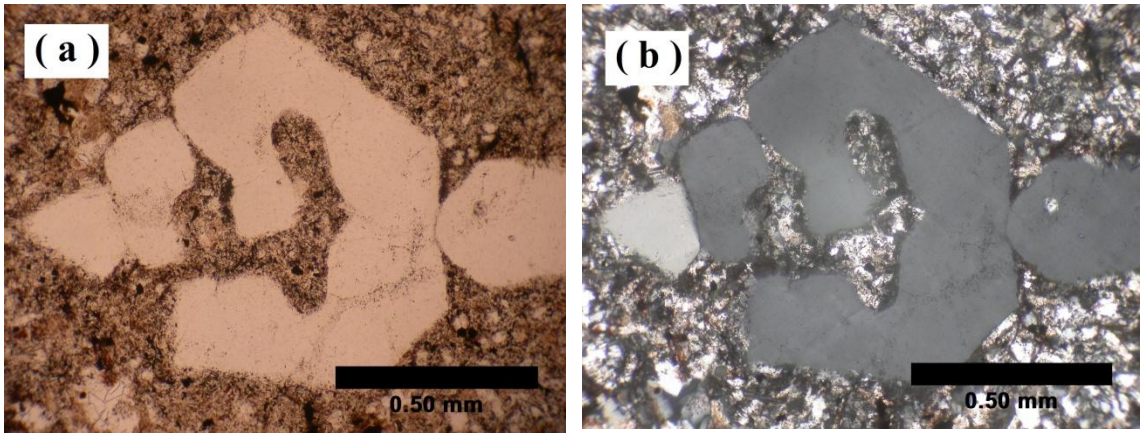

Figure 18: (a) plane-polarized photomicrograph and (b) cross-polarized photomicrograph.

(Circle# 3):

This is an example of a miarolitic cavity (Fig. 19).

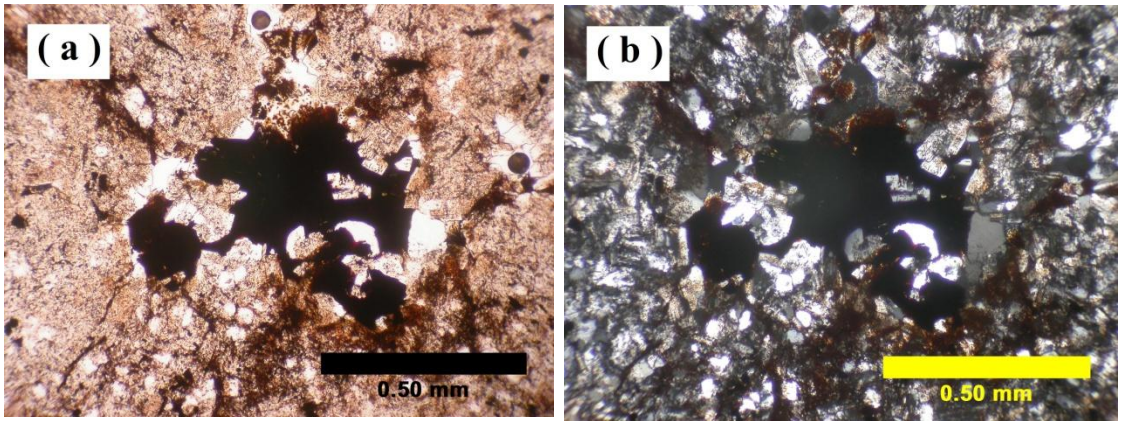

Figure 19: (a) plane-polarized photomicrograph and (b) cross-polarized photomicrograph.

(Circle# 4):

Figure 20 displays miarolitic cavity.

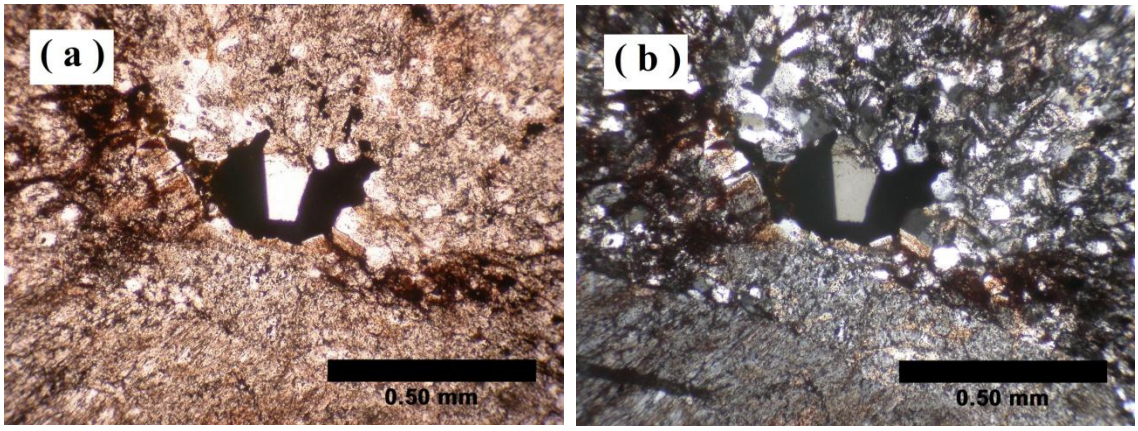

Figure 20: (a) plane-polarized photomicrograph and (b) cross-polarized photomicrograph.

SJ – 3 – a:

(Circle# 1):

This is an example of a hexagonal quartz crystal (Qtz) cut perpendicular to the C axis (fig.21).

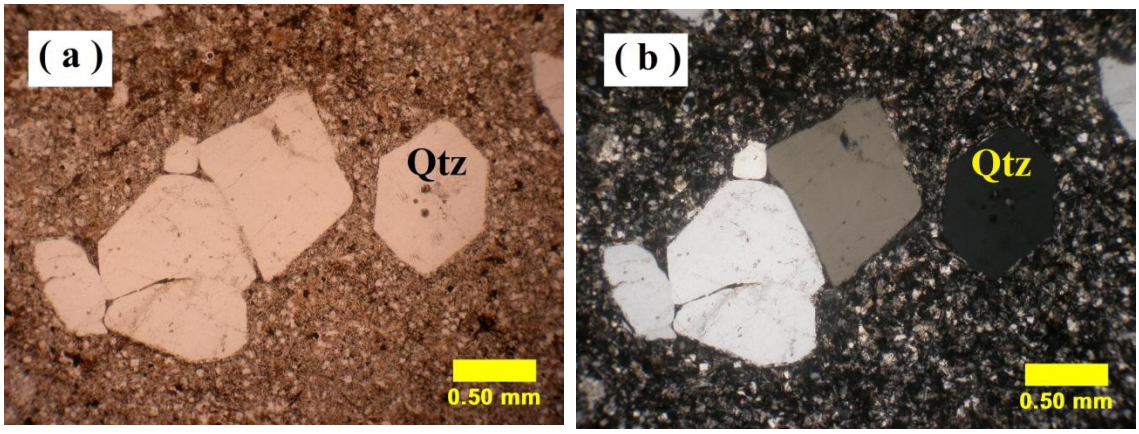

Figure 21: (a) plane-polarized photomicrograph and (b) cross-polarized photomicrograph.

(Circle# 2):

This is an example of a resorbed, clustered quartz phenocryst. Evidence of resorption is around the phenocryst (fig.22).

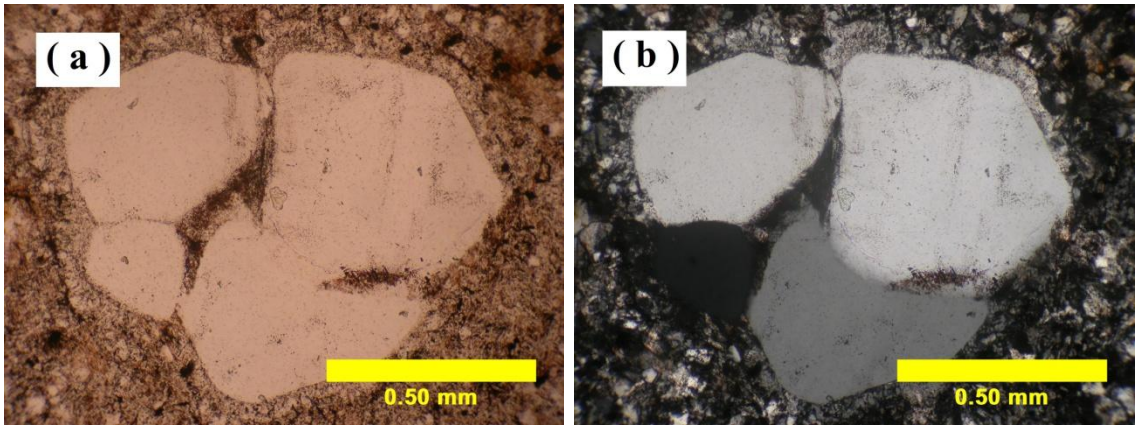

Figure 22: (a) plane-polarized photomicrograph and (b) cross-polarized photomicrograph.

(Circle# 3):

This is an example of a small euhedral quartz phenocryst with a perpendicular section to the C axis (fig. 23).

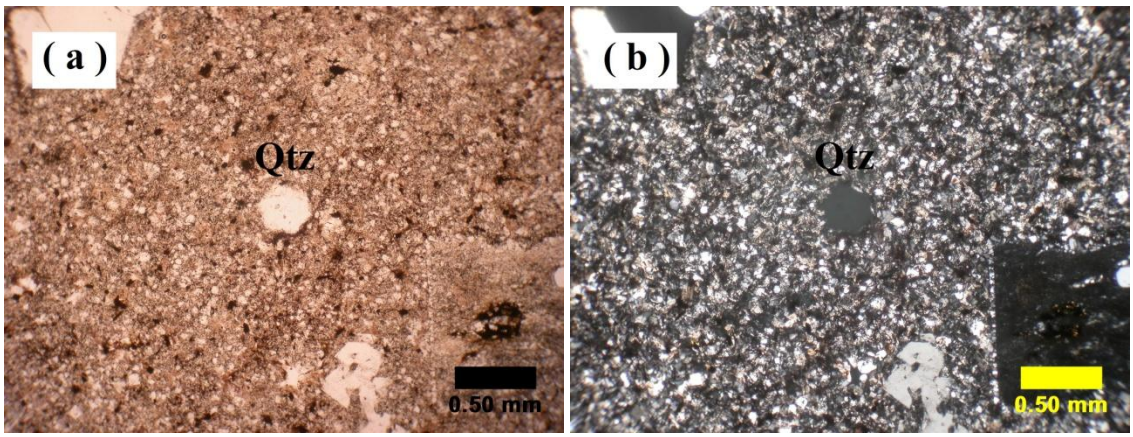

Figure 23: (a) plane-polarized photomicrograph and (b) cross-polarized photomicrograph.

(Circle# 4):

Figure 24 illustrates two miarolitic cavities with very small quartz crystals.

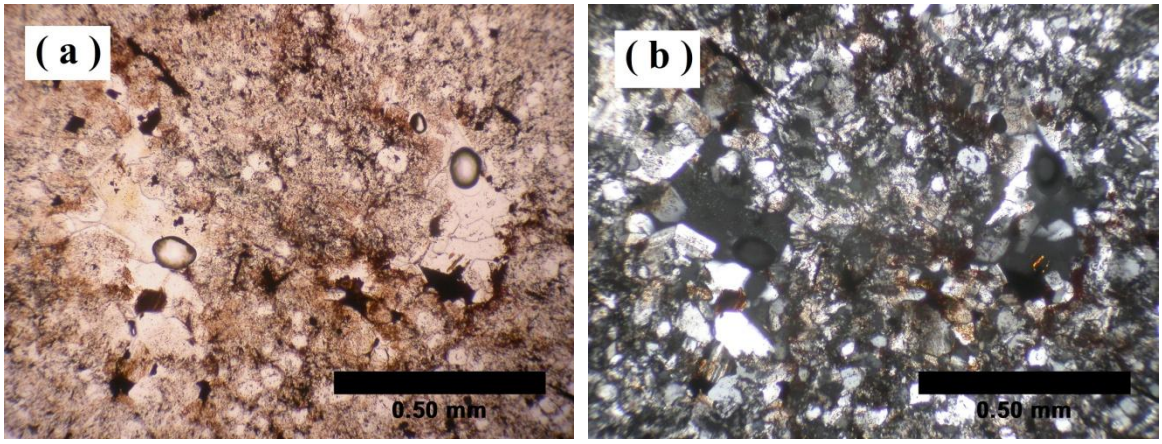

Figure 24: (a) plane-polarized photomicrograph and (b) cross-polarized photomicrograph.

(Circle# 5):

Figure 25 shows an example of a large subhedral quartz phenocryst.

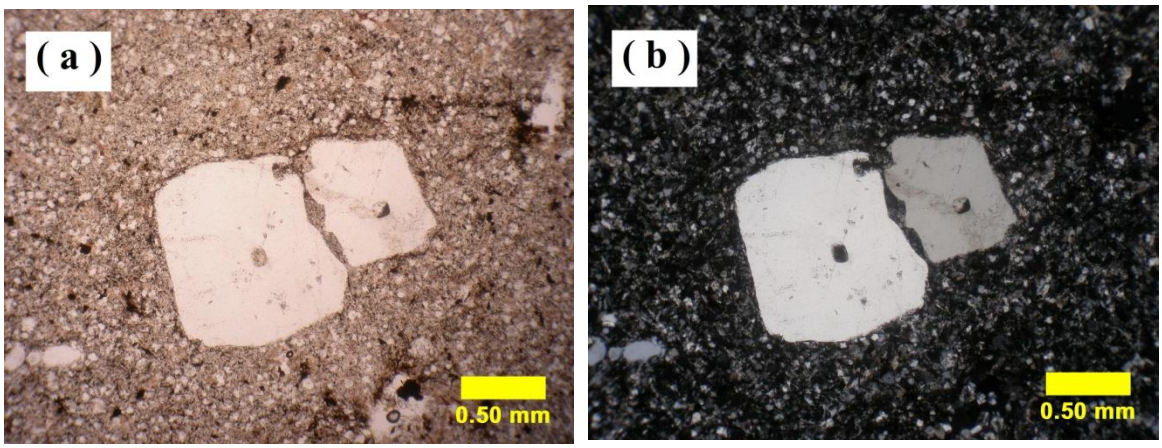

Figure 25: (a) plane-polarized photomicrograph and (b) cross-polarized photomicrograph.

APPENDIX B

CATHODOLUMINESCENCE PHOTOMICROGRAPHS

Selection Criteria for Cathodoluminescence CL

Euhedral crystals with sections perpendicular to the C axis possibly give the best zoning profile from core to rim as they avoid the problem of the "cut effect". Crystals that were representative of early and late growth of quartz are: 1) early – crystals that occur as inclusions in feldspar (very rare), and the largest crystals in the thin section; 2) late – crystals that are very small, similar to that of the size of the matrix but still phenocrysts, and crystals that are on the edge of miraloitic cavities (See figs. a-f).

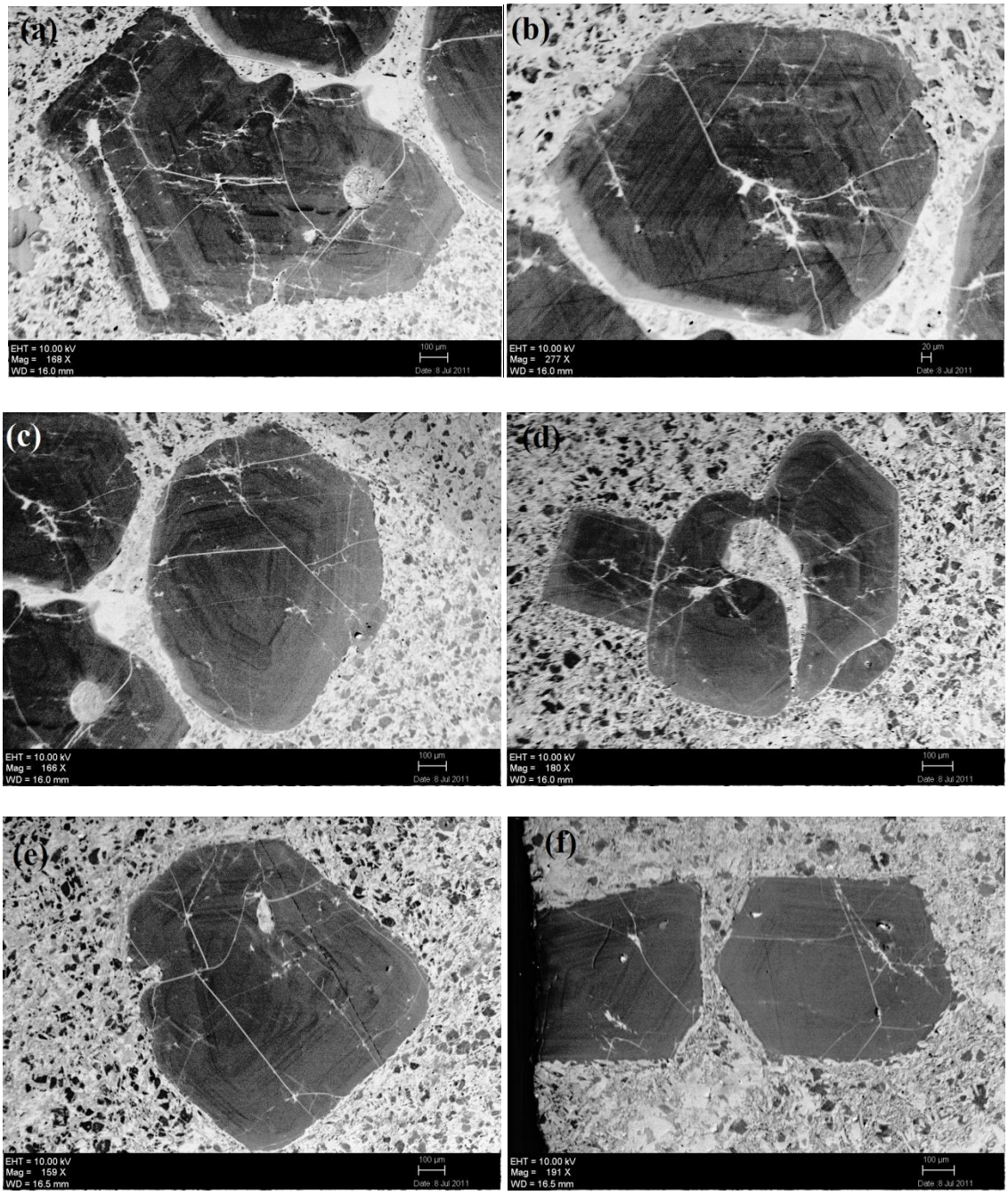

(Figures. a-f) Cathodoluminescence photomicrographs show quartz phenocrysts in a variety of phenocrysts types with obvious zonation.

APPENDIX C

TABLES

Table 1. Criteria that were used to pick what sections to polish:

A- Quartz included in feldspar.
B- Quartz large and euhedral crystals.
C- Quartz clusters crystals.
D- Quartz resorbed crystals.

Sample No.	A	B	C	D	Total	State of Sample
SJ - 1- a	0	4	5	0	9	no
SJ - 1- b	0	5	3	1	9	no
SJ - 1 - c	0	5	3	0	8	no
SJ - 1 - d	0	6	2	0	8	no
SJ - 1 - e	1	6	3	2	12	was sent
						no
SJ - 2 - a	0	5	5	2	12	no
SJ - 2 - b	1	5	4	1	11	was sent
SJ - 2 - c	0	4	3	1	8	no
SJ - 2 - d	0	4	1	1	6	no
SJ - 2 - e	0	6	3	0	9	no
						no
SJ - 3 - a	1	5	3	1	10	was sent
SJ - 3 - b	0	6	3	1	10	no
SJ - 3 - c	0	4	4	0	8	no
SJ - 3 - d	0	5	6	1	12	no
SJ - 3 - e	0	5	3	2	10	no
						no
SJ - 4 - a	0	6	2	2	10	no
SJ - 4 - b	0	5	2	2	9	no
SJ - 4 - c	0	7	5	3	15	no
SJ - 4 - d	0	4	4	2	10	no
						no
JH - 2 - 04a1	0	8	5	2	15	no
JH - 2 - 04a2	0	4	5	3	12	no
JH - 2 - 04b1	0	5	5	1	11	no
JH - 2 - 04b2	0	4	4	3	11	no
JH - 2 - 04c	0	8	4	4	16	was sent
JH - 2 - 04d	0	5	4	4	13	was sent
JH - 2 - 94	0	3	2	2	7	no

Table 2. The priority of Cathodoluminescence analysis

Sample #	First Priority	Second Priority	Third Priority	Fourth Priority	Fifth Priority
JH - 2 - 04c	**Circle# 1**	**Circle# 3**	**Circle# 4**	**Circle# 5**	**Circle# 2**
JH - 2 - 04d	**Circle# 1**	**Circle# 2**	**Circle# 3**	**Circle# 4**	**Circle# 5**
SJ - 1 - e	**Circle# 1**	**Circle# 2**	**Circle# 3**	**Circle# 4**	**Circle# 5**
SJ - 2 - b	**Circle# 1**	**Circle# 2**	**Circle# 4**	**Circle# 3**	
SJ - 3 - a	**Circle# 1**	**Circle# 2**	**Circle# 3**	**Circle# 5**	**Circle# 4**

BIBLIOGRAPHY

Gilbert, M. C. (1983). Timing and Chemistry of Igneous Event Associated With the Southern Oklahoma Aulacogen. *Tectonophysics 94*, 439-455.

Gilbert, M. C., & Hughes, S. S. (1986). Partial Chemical Characterization of Cambrian Basaltic Liquids of The Southern Oklahoma Aulacogen. *Pertology of the Cambrian Wichita Mountains Igneous Suite*, 73-79.

Gilbert, M. C., & Myers, J. D. (1986). Overview of the Wichita Granite Group. In: Gilbert, M. C. (ed.). *Petrology of the Cambrian Wichita Mountains Igneous Suite*, 107-116.

Gilbert, M. C., & Powell, B. N. (1988). Igneous Geology of the Wichita Mountains, Southwestern Oklahoma. *South-Central Section of the Geological Society of America*, 109-126.

Gilbert, M., & Hogan, J. P. (2010). Our favorite outcrop: The striking but engimatic granite-gabbro contact of the Wichita Mountains Igneous Province. *Shale Shaker*, 130-134.

Gotze, J., Plotze, M., & Habermann, D. (2001). Origin, spectral characteristics and practical applications of the cathodoluminescence (CL) of quartz - a review. *Mineralogy and Petrology*, 225-250.

Ham, W. E., Denison, R. E., & Merritt, C. A. (1964). Basement Rocks and Structure Evolution of Southern Oklahoma. *Oklahoma Geological Survey Bulletin 95*, 302.

Hames, W. E., Hogan, J. P., & Gilbert, M. C. (1995). Revised Granite-gabbro a Relatioships, Southern Oklahoma Aulacogen U.S.A. *12th International Conference on Basement Tectonics*, 44.

Higgins, M. D. (1998). Origin of Anorthosite by Textural Coarsening: Quantitative Measurements of a Natural Sequence of Textural Development. *Journal of Petrology*, 1307-1323.

Hoffman, P., Dewey, J., & Burke, K. (1974). Aulacogens and Their Genetic Relationship to Geosynclines,With a Proterozoic Example From The Great Slave Lake,. *Modern and Ancient Geosynclinal Sedimentation,*, 38-55.

Hogan, J. P. (1993). Monomineralic Glomerocrysts: Textural Evidence for Mineral Resorption During Crystallization of Igneous Rocks. *The Journal of geology*, 531-540.

Hogan, J. P., & Gilbert, M. C. (1995). The A-type Mount Scott Granite sheet: Importance of crustal magma traps. *Journal of Geophysical Research*, 15,779-15792.

Hogan, J. P., & Gilbert, M. C. (1997). Intrusive style of A-type sheet granites in a rift environment: the southern Oklahoma Aulacogen. *Geological Society of America*, 299-311.

Hogan, J. P., & Gilbert, M. C. (1998). The Southern Oklahoma Aulacogen: A Cambrian analog for Mid-Proterozoic AMCG (Anorthosite-Mangerite-Charnockite-Granite) complexes? *Basment Tectonics*, 39-78.

Hogan, J. P., & O'Donnell, S. P. (2008). Textural Analysis of a Rhyolite Dike of the Southern Oklahoma Aulacogen at Medicine Park, Oklahoma.

Jerram, D. A., Cheadle, M. J., & Philpotts, A. R. (2003). Quantifying the Building Blocks of Igneous Rocks: Are Clustered Crystal Frameworks the Foundation? *Journal of Petrology*, 2033-2051.

Kirkpatrick, R. J. (1975). Crystal Growth From the Melt: A review. *American Mineralogist*, 798-814.

Kuo, L. C., & Kirkpatrick, R. J. (1985). Kinetics of Crystal dissolution in The System Diopside-Foresterite-silica. *Am. Jour. Sci.*, 51-90.

Lambert, D. D., Unruh, D. M., & Gilbert, M. C. (1988). Rb-Sr and Sm-Nd Isotopic Study of The Glen Mountains Layerd Complex: Initiation of Rifting Within The Southern Oklahoma Aulacogen. *Geology 16*, 13-17.

Liang, Y. (1999). Diffusive Dissolution in Ternary System: Analysis with Applications to Quartz and Quartzite Dissolution in Molten Silicates. *Geochimica et Cosmochimica Acta 63*, 3983-3995.

Merritt, C., Ham, W. E., & Denison, R. E. (1965). Basement Rocks and Structural Evolution of Southern Oklahoma - a Summary. *AAPG Buletin*, 927-943.

Müller, A., Kerkhof, A. M., Behr, H.-J., Kronz, A., & Koch-Müller, M. (2010). The evolution of late-Hercynian granites and rhyolites documented by quartz – a review. *Earth and Environmental Science Transactions of the Royal Society of Edinburgh*, 185-204.

Nekvasil, H. (1991). Ascent of Felsic magmas and Formation of Rapakivi. *Am. Mineral.*, 1279-1290.

Powell, B. N., C., G. M., & Fischer, J. F. (1980). Lithostratigraphic Classification of Basement Rocks of The Wichita Province, Oklahoma. *Geological Society of America 91*, 1875-1994.

Price, J. D. (1998). Petrology of The Mount Scott Granite. *Geology and Geophysics*, 240.

Price, J. D., Hogan, J. P., & Gilbert, M. C. (1996). Investigation of Late Diabase Dikes at Lake Elmer Thomas Dam, Wichita Mountains, Oklahoma. *Geological Society of AmericaAbstract with Programs 28*, 59.

Schaeben, H., Boogaart, K. G., Mock, A., & Breitkreuz, C. (2002). Inherited Correlation in Crystal Size Distribution: Comment and Reply. *Geology 30*, 282-283.

Schwindlinger, K. R., & Alfred T. Anderson, J. (1989). Synneusis of Kilauea Iki olivines. *Contributions to Minerology and Petrology*, 187-198.

Swanson, S. E. (1977). Relation of Nucleation and Crystal-Growth Rate to The Development of Granitic Textures. *American Mineralogist 62*, 966-978.

Tilton, G. R., Wetherrill, G. W., & Davis, G. L. (1962). Mineral Ages From The Wichita and Arbuckle Mountains, Oklahoma, and The St. Francois Mountauns, Missouri . *Journal of Geophysical Research 67*, 4011-4019.

Tsuchiyama, A., & Takahashi, E. (1985). Melting Kinetics of a Plagioclase Feldspar. *Contrib. Mineral. Petrol.*, 345-354.

Vance, J. A. (1969). On Synneusis. *Contribution to Mineralogy and Petrology 24*, 7-29.

Vogt, J. H. (1921). The Physical Chemistry of The Crystallization and Magmatic Differentiation of The Igneous Rocks. *Journal of Geology 29*, 318-350.

Walderhaug, O., & Rykkje, J. (2000). Some examples of the effect of Cystallographic Orientation on the Cathodoluminescence Colors of Quartz. *Journal of Sedimentary Research 70*, 545-548.

Wark, D. A., & Stimac, J. A. (1990). Mantled Feldspars and "Spongy" Plagioclase in Volcanic Rocks: Origin by Alkali Exchange Across a Two Liquid Interface. *Trans. Am. Geophys. Union*, 665.

Wark, D., & Waston, E. (2006). The TitaniQ: a Titanium-in-Quartz Geothermometer. *Contrib. Mineral Petrol*, 743-754.

Waston, E. B. (1982). Basalt Contamination by Continental Crust: Some Experiments and Models. *Contrib. Mineral. Petrol.*, 73-87.

Watt, G. R., Wright, P., Galloway, S., & McLean, C. (1997). Cathodoluminescence and trace element zoning in quartz phenocrysts and xenocrysts. *Geochimica et Cosmochimica Acta*, 4337-4348.

Weaver, B. L., Cameron, M., & Medina, D. D. (1986). A Preliminary Report on Trace-Element Geochemistry of Igneous Rock of The Southern Oklahoma Aulacogen. *Oklahoma Geological Survey Guidebook 23*, 80-85.

Wiebe, R. A., Wark, D. A., & Hawkins, D. P. (2007). Insights from Quartz Cathodoluminescence Zoning into crystallization of the Vinalhaven Granite, Coastal Maine. *Contrib.Mineral Petrol*, 439-453.

Wright, J., Hogan, J. P., & Gilbert, M. C. (1996). The Southern Oklahoma Aulacogen: not just another B.L.I.P. *Eos, Transactions, American Geophysical Union 77*, 845.

VITA

Sedeg Ahmed E. Ahmed was born June 11, 1978 in Zawia, Libya. He received his Bachelor of Science degree in Geology from University of Aljabal Algharbi at Zawia, Libya in 2001. He has served as a Teaching Assistant in the Department of Geology at University of Aljabal Algharbi for four years. In August of 2009, he enrolled in the Graduate School at Missouri University of Science and Technology. In December 2011, he received his Masters in Geology and Geophysics from Missouri University of Science and Technology at Rolla, Missouri.